

Contents lists available at ScienceDirect

Transportation Research Part C

journal homepage: www.elsevier.com/locate/trc



Check for updates

Integrating public transit signal priority into max-pressure signal control: Methodology and simulation study on a downtown network

Te Xu*, Simanta Barman, Michael W. Levin, Rongsheng Chen, Tianyi Li

Department of Civil, Environmental, and Geo-Engineering, University of Minnesota, MN, USA

ARTICLE INFO

Keywords: Max-pressure control Maximum stability Public transit Bus rapid transit Transit signal priority

ABSTRACT

Max-pressure signal control has been analytically proven to maximize the network throughput and stabilize queue lengths whenever possible. Since there are many transit lines operating in the metropolis, the max-pressure signal control should be extended to multi-modal transportation systems to achieve more widespread usage. The standard max-pressure controller is more likely to actuate phases during high-demand approaches, which may end up ignoring the arrival of buses, especially in bus rapid transit. In this paper, we propose a novel max-pressure signal control that considers transit signal priority of bus rapid transit systems to achieve both maximum stability for private vehicles and reliable transit service. This study revises the original max-pressure control to include constraints that provide priority for buses. Furthermore, this policy is decentralized which means it only relies on it relies only on the local conditions of each intersection. We set the simulation on the real-world road network with bus rapid transit systems. Numerical results show that the max-pressure signal control which considers transit signal priority can still achieve maximum stability compared with other signal control integrated with transit signal priority. Furthermore, the max-pressure control reduces private vehicle travel time and bus travel time compared to the current signal control.

1. Introduction

As a bottleneck for urban transportation networks, intersections have attracted lots of attention from researchers. To optimize signal timing and achieve maximum throughput of intersections, recent studies have proposed max-pressure-based signal control policies for adaptive adjustive signal timings (Wuthishuwong and Traechtler, 2013; Varaiya, 2013; Gregoire et al., 2014; Xiao et al., 2014; Rey and Levin, 2019; Chen et al., 2020; Mercader et al., 2020; Levin et al., 2020; Li et al., 2021). One property of max-pressure control is it had proven to serve all demands whenever possible. Max-pressure control is also decentralized, which means the network-level optimal solution can be found by a local traffic signal controller only using the traffic information from upstream and downstream links (Varaiya, 2013; Tassiulas and Ephremides, 1990).

Implementation of max-pressure control faces some real-world challenges, such as the equity between private vehicle users and public transit users. Specifically, implementation of max-pressure control may cause bus service to become unreliable and increase bus users' travel time because the max-pressure controller is more likely to give phases for a large demand approach. However, bus service quality is an important factor that could promote part of the travel demand shift from driving to public transit. To achieve equity between different transportation modes, public transit priority is introduced to improve bus operation efficiency (Hunter-Zaworski et al., 1995; Ma et al., 2014; Ding et al., 2015; Anderson and Daganzo, 2020; Deng and Nelson, 2011; Eichler and Daganzo, 2006; Levinson et al., 2002; Bayrak and Guler, 2020; Wadjas and Furth, 2003; Yang et al., 2019). One major approach is granting

E-mail address: te000002@umn.edu (T. Xu).

^{*} Corresponding author.

signal timing priority (also called transit signal priority, TSP) to the buses, TSP has three kinds of types: passive priority method, active priority method, and real-time priority control method (Hunter-Zaworski et al., 1995; Currie and Shalaby, 2008; Christofa and Skabardonis, 2011; Li et al., 2011; Ma et al., 2014; Ding et al., 2015; Wadjas and Furth, 2003; Lin et al., 2019; Yang et al., 2019; Bayrak and Guler, 2020). The other major approach is designing exclusive bus lanes, which are usually built with bus rapid transit system (Deng and Nelson, 2011; Levinson et al., 2002; Eichler and Daganzo, 2006). For bus lanes, there are some other designing strategies, such as queue jumper lanes (Zhou and Gan, 2005; Truong et al., 2016) and intermittent bus lane (Eichler and Daganzo, 2006; Chiabaut et al., 2012; Chiabaut and Barcet, 2019; Currie and Lai, 2008). Both can effectively increase the operational speed of buses and increase the level of service of the public transit system.

However, previous max-pressure signal control policies assume that public transit uses the same signal timing as private vehicles. If the operation of public transit is ignored, there may be problems at certain intersections that are neglected when implementing max-pressure controller policies. For instance, the max-pressure controller is more likely to actuate phases for high-demand approaches, which may delay buses waiting in lower-demand approaches.

In order to improve the scope of the application of the max-pressure control policy, we combine the max-pressure control with TSP for the first time. The contributions of this paper are as follows: (1) We modify Varaiya's max-pressure control policy to give priority signals to bus rapid transit (Varaiya, 2013). Specifically, in this paper, we only consider situations where bus rapid transit has exclusive bus lanes. (2) We design dynamic queueing models for bus rapid transit systems and private vehicles. (3) We formulate the conflict region model, which is inspired by autonomous intersection control, for the proposed max-pressure policy to eliminate the conflicts between buses and private vehicles (Levin et al., 2019) (4) We analytically prove the max-pressure control policy considering bus rapid transit can also achieve optimal throughput at the network level. (5) We implement our simulation using the road network, bus rapid transit (BRT) system, and bus timetables from downtown Austin, Texas, USA.

2. Literature review

In this part, we first review related papers focusing on transit signal priority. Then we review the existing literature on max-pressure control.

2.1. Transit signal priority

Transit signal priority has been implemented in many cities around the world to improve bus operational performance (Hunter-Zaworski et al., 1995; Ma et al., 2014; Ding et al., 2015; Anderson and Daganzo, 2020). Many bus routes are located in a primary corridor of cites (Deng and Nelson, 2011). High-performance public transit systems can attract more travelers to transit from using private vehicles, which would reduce traffic emissions and congestion significantly. One way to enhance public transit priority is building exclusive bus lanes or intermittent bus lanes (Eichler and Daganzo, 2006; Chiabaut et al., 2012; Chiabaut and Barcet, 2019; Currie and Lai, 2008), which are part of bus rapid transit (BRT) Systems (Levinson et al., 2002; Eichler and Daganzo, 2006). Another way is designing TSP strategies for public transit systems. Passive priority methods (pre-determined signal setting) (Lin et al., 2019), active priority methods (real-time detection of buses on the intersection arms) (Currie and Shalaby, 2008; Christofa and Skabardonis, 2011; Lin et al., 2015), and adaptive/real-time priority control method are three types of the most widely used TSP strategies (Li et al., 2011). For passive priority signal, all the phases and timing are pre-designed to accommodate intersection traffic demand and buses operation. The green time extension is a typical method belonging to active transit signal priority, which required bus arrival information, such as arrival time, speed to insert phases for buses. Specifically, adaptive/real-time priority controllers are not only based on the information from detectors but also try to optimize signal timings for some performance metrics, like private vehicle delay, person delay, bus delay, etc.

Previous studies have tried to achieve more benefits from the implementation of TSP strategies. Some papers used simulation tools to test the performance of TSP (Chang et al., 2003; Wadjas and Furth, 2003; Dion et al., 2004; Stevanovic et al., 2008). Due to the complexity, these simulations only considered one intersection or arterial, rather than the whole road network. For instance, Stevanovic et al. (2008) used VISSIM and Direct CORSIM to optimize basic signal timing parameters for transit signal priority setting. Their results showed the transit signal priority setting based on a genetic algorithm can reduce travel delay on the corridors in Albany, NY, with mixed traffic and transit operations. With the development of intelligent transportation systems, several studies aimed to leverage advanced transportation technology to make the best use of TSP. Wu et al. (2020) analyzed the transit signal priority considering buses as moving bottlenecks along an arterial with mixed traffic scenarios. They used the lax-hopf equation (Claudel and Bayen, 2010a,b) to evaluate vehicle operations at the arterial level, the results showed that implementing TSP can be better than implementing exclusive bus lanes in some scenarios. Yang et al. (2019) used more precise and detailed information from connected vehicles for TSP implementation to minimize the delay of buses and cars. Bayrak and Guler (2020) tried to determine the optimal transit signal priority implementation locations in an urban transportation network. They tested different scenarios aiming to minimize the total travel time of network users. Some studies used simulation-based methods to explore the TSP. Meanwhile, optimization-based methods are also popular in improving TSP strategies. Ma et al. (2014) proposed a person-capacitybased optimization method for the transit priority operation at isolated intersections. Their optimization problem was formulated as a mixed integer linear program (MILP). Christofa et al. (2013) presented a person-based traffic responsive signal control system for TSP, which was formulated as a Mixed Integer Nonlinear Program (MINLP) aiming to minimize the total person delay while providing priority to public transit vehicles. Some data-driven based methods are also used in designing TSP strategies. Ding et al. (2015) established a multi-objective TSP method that used the ARIMA-SVM hybrid model to predict bus dwell time at bus stations.

The prediction model used data extracted from the BRT Line 2 from Changzhou City, China. With real-time average passenger delay, the maximum queue length, and the exhaust emissions as its optimization objectives, their proposed TSP method performed well in VISSIM simulation experiments.

Overall, existing studies of TSP have demonstrated that TSP strategies are an efficient way to improve the performance of public transit systems. These studies leveraged simulation-based and model-based methods to find the optimal locations, modified strategies to achieve better implementations with traditional vehicles. However, none of them consider the stable impacts for private vehicles. Furthermore, most of them focused only on one intersection, one bus line, or in some grid-based networks. Specifically, when TSP sacrifices the general benefits for private vehicles, the queue length of private vehicles may grow arbitrarily large around the urban network, which we call unstable scenarios.

2.2. Max-pressure control

Initially, max-pressure control was developed as a scheduling strategy in communication and power systems (Tassiulas and Ephremides, 1990). Varaiya (2013) converted it to a decentralized traffic signal control policy that guarantees network stability whenever possible based on the store-and-forward queueing model. In Varaiya (2013)'s paper, max-pressure control defines the pressures of each turning movement then finds the phase with the maximum pressure for each iteration. In addition, it is also a decentralized algorithm that can be computed separately for the individual intersection.

The advantageous properties of max-pressure control have led many researchers to introduce it into the area of traffic signal control (Wuthishuwong and Traechtler, 2013; Varaiya, 2013; Gregoire et al., 2014; Xiao et al., 2014; Rey and Levin, 2019; Chen et al., 2020; Mercader et al., 2020; Levin et al., 2020; Li et al., 2021). Varaiya (2013) defined the weight function as the difference between the queue length of the current movement and the weighted average queue length of downstream movements. Some researchers have followed Varaiya's weight calculations (Rey and Levin, 2019; Levin et al., 2020), while some others have used travel time instead of queue length to define the movement weight (Mercader et al., 2020). Li et al. (2021) used the density information and designed a position weighted back-pressure policy to calculate the weight. However, it is impossible to know spatial-time density in the real world due to the limitations of loop detectors. After calculating the weight of each movement, the pressure term can be calculated by the weights. Most papers calculated the pressure term from the product of link capacity and movement weight (Varaiya, 2013; Chen et al., 2020; Mercader et al., 2020; Levin et al., 2020; Li et al., 2021), while others calculated the pressure term from delay-based information (Wu et al., 2017).

Due to the complexity of the max-pressure control policy, some researchers did not include an analytical proof of stability. Sun and Yin (2018) used the VISSIM platform to compare several proposed max-pressure-based traffic signal control methods. The results showed that max-pressure control achieved better control performance of adaptive signal control systems. Also, the cycle-based max-pressure control seems to perform worse than the non-cyclic max-pressure control. Mercader et al. (2020) compared travel-time-based max-pressure controller with other traffic controllers via micro-simulation study. Their results showed that the max-pressure controller performs better than other traffic signal controllers in terms of travel delay.

Several improvements have been made to make the max-pressure control more palatable for practical implementation. Rey and Levin (2019) put attention on the long-time existence of mixed traffic flow and proposed a modified max-pressure traffic control policy for mixed traffic flow of legacy and autonomous vehicles. They introduced a blue phase to coordinate autonomous vehicles at network intersections. They also proved that the proposed hybrid network max-pressure controller can achieve maximum stability, i.e. maximizes throughout. Chen et al. (2020) developed the AIM-ped algorithm, which can achieve optimal throughput combined with max pressure control. Their paper proved that the max-pressure controller could achieve a more realistic implementation. To reduce the negative influence brought by the original max-pressure control police, Levin et al. (2020) introduced a cyclical phase structure max-pressure controller to make the max-pressure policy more friendly for drivers' preference. The most similar previous study to this one is the paper that considered pedestrians (Chen et al., 2020). However, their simulations were only implemented on the grid-based network. Inspired by the aforementioned research, we extend the max-pressure policy to consider the transit signal priority of bus rapid transit systems in the real-world network for the first time.

3. Network model

3.1. Road network model

Consider a road network $\mathcal{G} = (\mathcal{N}, \mathcal{A})$ with nodes \mathcal{N} and links \mathcal{A} . Nodes represent intersection locations. The link set \mathcal{A} is divided into three subsets, which is the entry link set \mathcal{A}_e , internal link set \mathcal{A}_i , and the exit link set \mathcal{A}_o . Entry links are the source links where buses and private vehicles can enter the network. Exit links are the sink links where buses and private vehicles leave the network. Internal links connect the intersections located inside the network. Note that the bus links in this paper only represent exclusive bus lanes (private vehicles are not allowed to use them), which are part of bus rapid transit systems in reality. We use Γ_i^+ and Γ_j^- to represent the sets of outgoing links and incoming links of intersections respectively. One turning movement is a combination of two links. For instance, (i,j) and (j,k) are two movements respectively. We define \mathcal{M} to be the set of all turning movements in the network. Let $x_{ij}^p(t)$ be the number of private vehicles on link i waiting to move to link j, and let $x_{ij}^B(t)$ be the number of buses waiting on link i waiting to move to link j. Let $d_i(t)$ be the demand entering the network on link $i \in \mathcal{A}_e$, which is composed by the bus demand $d_i^B(t)$ and private vehicles' demand $d_i^P(t)$. Turning proportion $r_{jk}^B(t)$ is the proportion of buses entering j that will next move to k. We assume that $r_{ij}^B(t)$ is fixed (we could get this information from the bus company or do field surveys), which

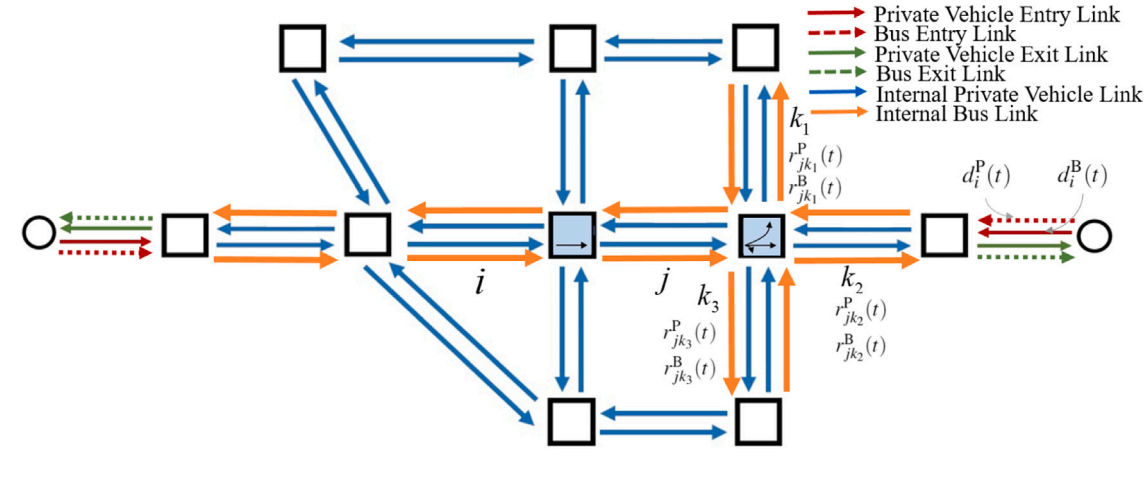


Fig. 1. Network example.

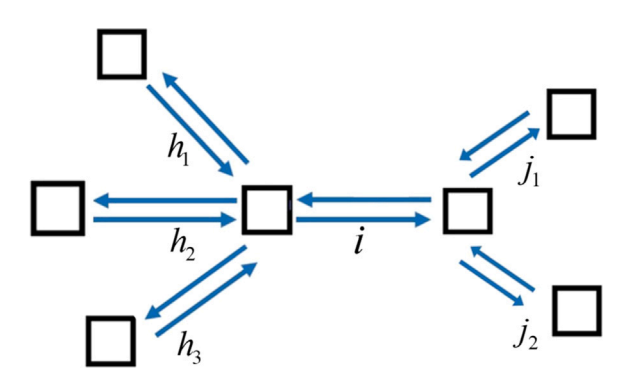


Fig. 2. Queue evolution instruction.

represents turning movements of buses. Turning proportion $r_{jk}^P(t)$ determines the proportion of private vehicles entering j that will next move to k, which are independent identically distributed random variables with mean \bar{r}_{ij}^P . We separate the link queues by turning movements since different turning movements at intersections could not be activated at the same time in some scenarios. The capacity of bus link i is denoted by Q_i^B . Therefore $Q_{ij}^B = \min(Q_i^B, Q_j^B)$, is the maximum number of buses that can move from i to j in one time step. The capacity of private vehicle link i is denoted by Q_i^P . Therefore, $Q_{ij}^P = \min(Q_i^P, Q_j^P)$, is the maximum flow of vehicle movement (i, j). Note that, both the buses' and private vehicles' capacities represent the physical properties of the road, which means they are determined value. We assume that Q_{ij}^P and Q_{ij}^P are constants. These variables are shown in Fig. 1.

3.2. Bus queueing model

To represent the propagation of bus queueing in the network, we use the store-and-forward model of Varaiya (2013). We assume buses have entry and exit links. For the internal links, we have the following equations to represent flow conservation:

$$x_{ij}^{B}(t+1) = x_{ij}^{B}(t) - y_{ij}^{B}(t) + \sum_{(i,j,h) \in \mathcal{A}^{3}} y_{hi}^{B}(t) \times r_{ij}^{B}(t)$$
 (1)

where $y_{ij}^{\rm B}(t)$ is the number of buses from i to j at time t, which is controlled by traffic signal. $r_{ij}^{\rm B}(t)$ is the proportion of buses entering i that will next move to j. Fig. 2 shows how the queue evolves from upstream to downstream. Flow conservation also applies to entry links, which are connected with bus terminal stations.

$$x_{ii}^{B}(t+1) = x_{ii}^{B}(t) - y_{ii}^{B}(t) + d_{i}^{B}(t) \times r_{ii}^{B}(t)$$
(2)

We assume that entry link $i \in A_e$, $d_i^B(t)$ is based on the bus timetables. In reality, the number of buses from terminal stations is varies over time throughout the day. We denote the mean value of bus entering flow as \bar{d}_i^B and further assume $d_i^B(t)$ has maximum value \bar{d}_i^B . Intersection-controlled bus movement flow is $y_{ij}^B(t)$. At each time step, a traffic signal phase is selected. The activation of

bus turning movement (i, j) is denoted by $s_{ij}(t) \in \{0, 1\}$. $s_{ij}(t) = 1$ means movement (i, j) gets a green light, and $s_{ij}(t) = 0$ means that movement (i, j) gets a red light. The value of $y_{ij}^B(t)$ is determined by the following equation

$$y_{ij}^{B}(t) = \min \left\{ Q_{ij}^{B} s_{ij}(t), x_{ij}^{B}(t) \right\}$$
(3)

3.3. Private vehicle queueing model

To represent the propagation of private vehicles queueing in the network, we use the store-and-forward model from Varaiya (2013). We assume private vehicles also have entry and exit links. For the internal links, we have the following equations:

$$x_{ij}^{P}(t+1) = x_{ij}^{P}(t) - y_{ij}^{P}(t) + \sum_{(i,j,h) \in \mathcal{A}^{3}} y_{hi}^{P}(t) \times r_{ij}^{P}(t)$$
(4)

where $y_{ij}^{P}(t)$ is the flow of private vehicles from i to j at time t, which is controlled by traffic signal. $r_{ij}^{P}(t)$ is the proportion of private vehicles entering i that will next move to j. Fig. 2 shows how the queue of private vehicles evolves from upstream to downstream. Flow conservation also applies to entry links, but entering flow is determined by the demand $d_i^P(t)$.

$$x_{ii}^{P}(t+1) = x_{ii}^{P}(t) - y_{ii}^{P}(t) + d_{i}^{P}(t) \times r_{ii}^{P}(t)$$
(5)

We assume that for entry link $i \in A_e$, $d_i^P(t)$ all t are independent identically distributed random variables with mean \bar{d}_i^P . We further assume $d_i^P(t)$ has maximum value \tilde{d}_i^P .

Intersection controlled flow of private vehicles is $y_{ij}^p(t)$. At each time step, a traffic signal phase is selected. The activation of private vehicle turning movement (i,j) is denoted by $s_{ij}(t) \in \{0,1\}$. $s_{ij}(t) = 1$ means movement (i,j) gets a green light, and $s_{ij}(t) = 0$ means that movement (i,j) gets a red light. Noted that buses have priority in the intersections, which means if buses and private vehicles arrive at an intersection at the same time, traffic signal phases will choose 1 for buses and 0 for private vehicles. The value of $y_{ij}^p(t)$ is determined by the following equation

$$y_{ij}^{P}(t) = \min \left\{ Q_{ij}^{P} s_{ij}(t), x_{ij}^{P}(t) \right\}$$
 (6)

Furthermore, we can rewrite Eqs. (4) and (5) as the following two equations, respectively.

$$x_{ij}^{P}(t+1) = x_{ij}^{P}(t) - \min\left\{Q_{ij}^{P}s_{ij}(t), x_{ij}^{P}(t)\right\} + \sum_{h \in \mathcal{A}_{i}^{-}} \min\left\{Q_{hi}^{P}s_{ij}(t), x_{hi}^{P}(t)\right\} \times r_{ij}^{P}(t) \quad \forall i \in \mathcal{A}_{i}, j \in \mathcal{F}_{i}^{+}$$
 (7)

$$x_{ij}^{P}(t+1) = x_{ij}^{P}(t) - \min\left\{Q_{ij}^{P}s_{ij}(t), x_{ij}^{P}(t)\right\} + d_{i}^{P}(t) \times r_{ij}^{P}(t) \quad \forall i \in \mathcal{A}_{e}, j \in \Gamma_{i}^{+}$$
(8)

3.4. Signal control and transit signal priority

The activation of turning movement for buses and private vehicles is denoted by $s_{ij}(t) \in \{0,1\}$. Let $S_r(t)$ be an intersection matrix for intersection r, and all turning movements activated in intersection control $S_r(t)$ matrix cannot conflict with each other. Activating $S_r(t)$ at all time step, we can define the intersection control sequence $S_r = \{S_r(t), t \in T\}$ that includes signal controls for all intersections r from start to end. Let S be a set that includes all feasible network control matrices for all intersections, and S_r denotes a set including all feasible intersection matrices for intersection r. We denote the convex hull of all feasible signal control matrices as Conv(S).

We give public transit more priority than private vehicles when there are bus lanes with BRT, which means when the buses of BRT are waiting at an intersection constructed with bus lanes, the green light will be actuated to at least one phase of bus queues at the bus lanes. More specifically, the feasible signal control integrated with transit signal priority should obey the following relationships: First, the number of signal control buses flow $y_{ij}^B(t)$ should larger than zero if buses are waiting. That is

$$y_{ij}^{B}(t) = \min \left\{ Q_{ij}^{B} s_{ij}(t), x_{ij}^{B}(t) \right\} > 0 \qquad \text{if } \sum_{(i,j) \in \mathcal{A}^{2}} x_{ij}^{B}(t) > 0$$
 (9)

In order to activate the phases where the buses will travel through, we have the following equation

$$\sum_{(i,j)\in\mathcal{A}^2} s_{ij}(t) \times x_{ij}^{\mathrm{B}}(t) > 0 \qquad \text{if } \sum_{(i,j)\in\mathcal{A}^2} x_{ij}^{\mathrm{B}}(t) > 0 \tag{10}$$

After that, we rewrite Eq. (10) as follows

$$\sum_{(i,j)\in\mathcal{A}^2} s_{ij}(t) \times x_{ij}^{\rm B}(t) - 1 \ge 0 \qquad \text{if } \sum_{(i,j)\in\mathcal{A}^2} x_{ij}^{\rm B}(t) > 0 \tag{11}$$

Fig. 3 shows how the transit signal priority provide for a given fixed-time signal control, adaptive signal control, and max-pressure signal control.

Therefore, we can obtain some feasible signal controls $s_{ij}(t)$ that satisfy transit signal priority constraints, that is $s_{ij}(t) \in S_p$. We define S_p be a set that includes all feasible network controls integrated with transit signal priority. S_p is a subset of S, that is $S_p \subseteq S$. Furthermore, we define the convex hull of all feasible signal control integrated transit signal priority matrices as $Conv(S_p)$. For any

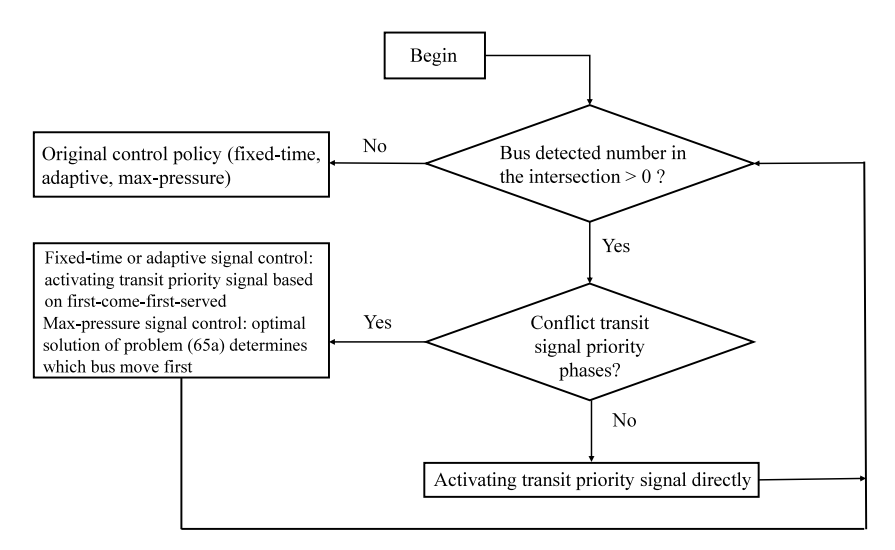


Fig. 3. Transit signal priority.

given intersection control sequence, the long-term average time used for serving turning movement (i, j), which also considers transit signal priority can be calculated by Eq. (12). Let \bar{s} and s(t) be the vectors of \bar{s}_{ij} and $s_{ij}(t)$ respectively.

$$\bar{s}_{ij} = \lim_{T \to \infty} \frac{1}{T} \sum_{t=1}^{T} s_{ij}(t) \tag{12}$$

The convex hull of S_p , the set of feasible network controls integrated with transit signal priority, is

$$\operatorname{Conv}(S_p) = \left\{ \sum_{s \in S} \lambda_s S \middle| \lambda_s S \le 0, \sum_{s \in S} \lambda_s = 1 \right\}$$
(13)

Proposition 1. If $s(t) \in S_p$ then there exists a $\bar{s} \in Conv(S_p)$ such that

$$\bar{\mathbf{s}} = \lim_{T \to \infty} \frac{1}{T} \sum_{t=1}^{T} \mathbf{s}(t) \tag{14}$$

Proof. First, we prove that $\bar{\mathbf{s}}$ is in the convex hull of S_p . For any T, Let $T \times \lambda_s$ be the number of times so that $\mathbf{s}(t) = \mathbf{s}$. Since $\mathbf{s}(t) \in S_p$, $\sum_{\mathbf{s} \in S_p} T \lambda_s = T$, so λ_s is the proportions of time spent in each phase. Therefore

$$\bar{\mathbf{s}} = \lim_{T \to \infty} \frac{1}{T} \sum_{t=1}^{T} \mathbf{s}(t) \tag{15}$$

$$= \lim_{T \to \infty} \frac{1}{T} \sum_{t=1}^{T} \sum_{\mathbf{s} \in S_n} \mathbb{I}(\mathbf{s}(t) = \mathbf{s})\mathbf{s}$$
 (16)

$$= \lim_{T \to \infty} \frac{1}{T} \sum_{t=1}^{T} \sum_{s \in S_n} T \lambda_s s \tag{17}$$

$$=\sum_{\mathbf{s}\in S_n}\lambda_{\mathbf{s}}\mathbf{s}\tag{18}$$

Since $\bar{\mathbf{s}}$ is the convex hull of \mathcal{S}_p , there exists $\lambda_{\mathbf{s}}$ satisfying $\sum_{\mathbf{s} \in \mathcal{S}_p} \lambda_{\mathbf{s}} = 1$ such that

$$\bar{\mathbf{s}} = \sum_{\mathbf{s} \in S_p} \lambda_{\mathbf{s}} \mathbf{s} \tag{19}$$

Define the indicator function as

$$\mathbb{I}(\mathbf{s}(t) = \mathbf{s}) \begin{cases} 1 & \text{if } \mathbf{s}(t) = \mathbf{s} \\ 0 & \text{if } \mathbf{s}(t) \neq \mathbf{s} \end{cases}$$
 (20)

For any $\lambda_s \in \{0,1\}$ there exists a sequence $\lambda_s(t)$ such that

$$\lim_{T \to \infty} \frac{1}{T} \sum_{t=1}^{T} \mathbb{I}(\mathbf{s}(t) = \mathbf{s}) = \lambda_{\mathbf{s}}$$
 (21)

Since $\sum_{s \in S_n} \lambda_s = 1$,

$$\lim_{T \to \infty} \frac{1}{T} \sum_{t=1}^{T} \mathbb{I}(\mathbf{s}(t) = \mathbf{s}) = 1$$
 (22)

Finally, we obtain the following equation

$$\bar{\mathbf{s}} = \lim_{T \to \infty} \frac{1}{T} \sum_{t=1}^{T} \sum_{\mathbf{s} \in S_n} \mathbb{I}(\mathbf{s}(t) = \mathbf{s})\mathbf{s} = \lim_{T \to \infty} \frac{1}{T} \sum_{t=1}^{T} \mathbf{s}(t) \quad \Box$$
(23)

3.5. Stable network

Stability refers to the ability to serve all demand in the transportation network. The bus transit rapid system is always stable since the number of buses belonging to the bus transit rapid system is limited and much smaller than the number of private vehicles. We define the *stability* of the network mathematically as follows:

Definition 1. The network is stable if the number of private vehicles remains bounded in expectation, i.e. there exists a $\kappa < \infty$ such that

$$\lim_{T \to \infty} \sup \left\{ \frac{1}{T} \sum_{t=1}^{T} \sum_{(i,j) \in \mathcal{A}^2} \mathbb{E}\{x_{ij}^{\mathsf{P}}(t)\} \right\} \le \kappa \tag{24}$$

It is easy to choose a demand rate vector \mathbf{d}^P such that no traffic signal timing policy can stabilize it. For instance, we can choose a very large demand rate that exceeds the turning movement capacity. The objective of our modified max-pressure control is to stabilize any private vehicles' demand rate that could be stabilized by some signal control also considering transit signal priority of bus rapid transit. To prove the maximum-stability property, we must first define analytically the sets of demands that could be stabilized. The definition is similar to that of Varaiya (2013) and Levin et al. (2020), but we should consider transit signal priority in this study.

3.6. Stable region

For private vehicles, since the demand of private vehicles is stochastic, the stable region is defined in terms of the average demand rates $\bar{\mathbf{d}}^P$. Demand for entry links can be propagation to demand for entry links. Let \mathbf{f}^P be the average private vehicle traffic volume for link i. For entry links, we have

$$f_i^P = \bar{d}_i^P \tag{25}$$

For internal links of private vehicles, $f_i^{\rm P}$ can be determined by conservation of flow:

$$f_j^{\mathrm{P}} = \sum_{i \in A} f_i^{\mathrm{P}} \bar{r}_{ij}^{\mathrm{P}} \tag{26}$$

By Proposition 1 of Varaiya (2013), for every demand rate $\bar{\mathbf{d}}^P$ and turning proportions $\bar{\mathbf{r}}^P$, there exists an unique average flow vector \mathbf{f}^P . The network can be stabilized if the average private vehicle traffic flow can still be served by some traffic signals integrated with transit signal priority. That is, there must exist an average signal activation $\bar{\mathbf{s}} \in \operatorname{Conv}(S_p)$. Note that, the stable region is different from Varaiya's definition (Varaiya, 2013), because the $\bar{\mathbf{s}} \in \operatorname{Conv}(S_p)$, which includes transit signal priority.

$$f_i^{\mathrm{P}} \bar{r}_{ij}^{\mathrm{P}} \le \bar{s}_{ij} \mathcal{Q}_{ij}^{\mathrm{P}} \tag{27}$$

where \bar{s}_{ij} can be obtained from Eq. (12), based on some feasible signal control consider bus priority $s_{ij}(t) \in S_p$.

Let \mathcal{D} be the set of demands which satisfy constraints (25)–(27). Let \mathcal{D}^0 be the interior of \mathcal{D} , where constraint (27) holds with strict inequality. Then there exists an $\epsilon > 0$ such that

$$f_i^P \bar{r}_{ij}^P - \bar{s}_{ij} Q_{ij}^P \le -\epsilon \tag{28}$$

Proposition 2. If $\bar{\mathbf{d}}^{\mathrm{P}} \notin \mathcal{D}$, then there does not exist a signal control policy can stabilize the network.

Proof. Since $\bar{\mathbf{d}}^P \notin \mathcal{D}$, $\forall \bar{s}_{ij} \in S_p$, there exists a $\theta > 0$ and at least one turning movement (i,j) satisfying $f_j^P \bar{r}_{ij}^P \geq \bar{s}_{ij} Q_{ij}^P + \theta$. Based on Eq. (4) we have

$$x_{ij}^{P}(t+1) - x_{ij}^{P}(t) = \sum_{(i,j,h) \in A^{3}} y_{hi}^{P}(t)r_{ij}^{P}(t) - y_{ij}^{P}(t)$$
(29)

Based on Eq. (29) we can obtain the following relationship:

$$\mathbb{E}\left[\sum_{t=0}^{\tau-1} \sum_{(i,j)\in\mathcal{A}^2} \left(x_{ij}^{P}(t+1) - x_{ij}^{P}(t)\right)\right] = \mathbb{E}\left[\sum_{(i,j)\in\mathcal{A}^2} \left(x_{ij}^{P}(\tau) - x_{ij}^{P}(0)\right)\right]$$
(30)

$$= \mathbb{E}\left[\sum_{t=0}^{\tau-1} \sum_{(h,i,j)\in\mathcal{A}^3} \left(y_{hi}^{P}(t)r_{ij}^{P}(t) - y_{ij}^{P}(t)\right)\right]$$
(31)

$$= \mathbb{E}\left[\sum_{(i,j)\in\mathcal{A}^2} \left(f_j^P \bar{r}_{ij}^P - \bar{s}_{ij} Q_{ij}^P\right)\right] \tag{32}$$

$$\geq \mathbb{E}\left[\tau\theta\right] = \tau\theta \tag{33}$$

Moving $x_{ii}^{P}(0)$ to the right hand side, we obtain:

$$\mathbb{E}\left[\sum_{(i,j)\in\mathcal{A}^2} x_{ij}^{P}(\tau)\right] \ge \theta\tau + \mathbb{E}\left[\sum_{(i,j)\in\mathcal{A}^2} x_{ij}^{P}(0)\right] \tag{34}$$

or equivalently

$$\mathbb{E}\left[\left|\mathbf{x}^{P}(\tau)\right|\right] \ge \theta\tau + \mathbb{E}\left[\left|\mathbf{x}^{P}(0)\right|\right] \tag{35}$$

From Eq. (35), we obtain

$$\lim_{T \to \infty} \mathbb{E}\left[\frac{1}{T} \sum_{t=1}^{T} |\mathbf{x}^{P}(t)|\right] \ge \lim_{T \to \infty} \mathbb{E}\left[\frac{1}{T} \sum_{t=1}^{T} \left[\theta t + \mathbb{E}\left[|\mathbf{x}^{P}(0)|\right]\right]\right]$$

$$= \lim_{T \to \infty} \mathbb{E}\left[\frac{1}{T} \sum_{t=1}^{T} \left[\theta t\right] + \lim_{T \to \infty} \mathbb{E}\left[\frac{1}{T} \sum_{t=1}^{T} \left[|\mathbf{x}^{P}(0)|\right]\right] = \infty$$
(36)

which violates Eq. (24).

Note that if the network is unstable, the private vehicle's turning movement flow is greater than the traffic signal integrated with transit priority that can serve.

3.7. Stability analysis based on average signal control

We now proceed to prove that the average signal control with bus priority will stabilize any private vehicle demand $\bar{\mathbf{d}}^P \in \mathcal{D}^0$. Since any demand $\bar{\mathbf{d}}^P \notin \mathcal{D}$ cannot be stabilized by Proposition 2, this essentially proves that we can find an average signal control to achieve stability. The only excluded demand is on the boundary of \mathcal{D} , for which the Markov chain can be shown to be null recurrent but not positive recurrent. Note that we only care about the stability of private vehicles because we always give signal priority to BRT.

Lemma 1. When $\bar{\mathbf{d}}^P \in \mathcal{D}^0$, the average signal control resulting from Eq. (12) and satisfying constraints (25)–(27) are used, there exists a Lyapunov function $v(t) \geq 0$ and constants $\kappa < \infty$, $\varepsilon > 0$ such that

$$\mathbb{E}\left[v(t+1) - v(t)|\mathbf{x}^{P}(t)\right] \le \kappa - \epsilon |\mathbf{x}^{P}(t)| \tag{37}$$

Proof. To calculate the queue length at time t + 1, we apply the private vehicle queueing models shown in Eq. (7)–(8). Then, let $\delta_{ij}(t)$ be the difference of the queue length of private vehicles between time steps t and time steps t + 1.

$$\delta_{ij}(t) = x_{ij}^{P}(t+1) - x_{ij}^{P}(t)$$

$$= -\min\left\{Q_{ij}^{P}s_{ij}(t), x_{ij}^{P}(t)\right\} + \sum_{h \in A^{-}} \min\left\{Q_{hi}^{P}s_{ij}(t), x_{hi}^{P}(t)\right\} \times r_{ij}^{P}(t) \quad \forall i \in \mathcal{A}_{i}, j \in \Gamma_{i}^{+}$$
(38)

$$\delta_{ij}(t) = x_{ij}^{P}(t+1) - x_{ij}^{P}(t) = -\min\left\{Q_{ij}^{P}s_{ij}(t), x_{ij}^{P}(t)\right\} + d_{i}^{P}(t) \times r_{ij}^{P}(t) \quad \forall i \in \mathcal{A}_{e}, j \in \Gamma_{i}^{+}$$
(39)

Let $\mathbf{x}^{P}(t)$ be the matrix including all queue length of private vehicles. We define the Lyapunov function v(t) as follows:

$$v(t) = \left| \mathbf{x}^{\mathbf{P}}(t) \right|^2 = \sum_{(i,j) \in \mathcal{A}^2} \left(x_{ij}^{\mathbf{P}}(t) \right)^2 \tag{40}$$

Then we expand the difference $v_1(t+1) - v_1(t)$:

$$v(t+1) - v(t) = \left| \mathbf{x}^{P}(t+1) \right|^{2} - \left| \mathbf{x}^{P}(t) \right|^{2} = \left| \mathbf{x}^{P}(t) + \delta(t) \right|^{2} - \left| \mathbf{x}^{P}(t) \right|^{2} = 2\mathbf{x}^{P}(t)^{T}\delta(t) + \left| \delta(t) \right|^{2}$$
(41)

$$2\mathbf{x}^{P}(t)^{T}\boldsymbol{\delta}(t) = -2x_{ij}^{P}(t)\sum_{i\in\mathcal{A}}\sum_{j\in\Gamma_{i}^{+}}\min\left\{Q_{ij}^{P}s_{ij}(t), x_{ij}^{P}(t)\right\} + 2\sum_{h\in\Gamma_{i}^{-}}\sum_{i\in\mathcal{A}}\sum_{j\in\Gamma_{i}^{+}}x_{ij}^{P}(t)\min\left\{Q_{hi}^{P}s_{hi}(t), x_{hi}^{P}(t)\right\}r_{ij}^{P}(t) + 2\sum_{i\in\mathcal{A}_{e}}\sum_{j\in\Gamma_{i}^{+}}\left(-\min\left\{Q_{ij}^{P}s_{ij}(t), x_{ij}^{P}(t)\right\} + d_{i}^{P}(t) \times r_{ij}^{P}(t)\right)$$

$$(42)$$

$$=2\sum_{i\in\mathcal{A}_{i}\cup\mathcal{A}_{e}}\sum_{j\in\Gamma_{i}^{+}}\min\left\{Q_{ij}^{P}s_{ij}(t),x_{ij}^{P}(t)\right\}\left(-x_{ij}^{P}(t)+\sum_{k\in\Gamma_{i}^{+}}r_{jk}^{P}(t)x_{jk}^{P}(t)\right) + 2\sum_{i\in\mathcal{A}_{e}}\sum_{j\in\Gamma_{i}^{+}}d_{i}^{P}(t)\times r_{ij}^{P}(t)\times x_{ij}^{P}(t)$$

$$(43)$$

Replacing the turning proportion $r_{ij}^{\mathrm{P}}(t)$ with average value $\bar{r}_{ij}^{\mathrm{P}}$, since $\lim_{T\to\infty}\frac{1}{T}\sum_{t=1}^{T}\sum_{(i,j)\in\mathcal{A}^2}r_{ij}^{\mathrm{P}}(t)=\sum_{(i,j)\in\mathcal{A}}\bar{r}_{ij}^{\mathrm{P}}$ since $r_{ij}^{\mathrm{P}}(t)$ is a random variable. Therefore we have the following equation:

$$\mathbb{E}\left[\mathbf{x}^{\mathbf{P}}(t)^{\mathrm{T}}\boldsymbol{\delta}(t)|\mathbf{x}^{\mathbf{P}}(t)\right] = \sum_{i \in \mathcal{A}_{i} \cup \mathcal{A}_{e}} \sum_{j \in \Gamma_{i}^{+}} \mathbb{E}\left[\min\left\{Q_{ij}^{\mathbf{P}}s_{ij}(t), x_{ij}^{\mathbf{P}}(t)\right\} \times \left(-x_{ij}^{\mathbf{P}}(t)\right)|\mathbf{x}^{\mathbf{P}}(t)\right] + \sum_{i \in \mathcal{A}_{i} \cup \mathcal{A}_{e}} \sum_{j \in \Gamma_{i}^{+}} \mathbb{E}\left[\min\left\{Q_{ij}^{\mathbf{P}}s_{ij}(t), x_{ij}^{\mathbf{P}}(t)\right\} \left|\mathbf{x}^{\mathbf{P}}(t)\right] \times \left(\sum_{k \in \Gamma_{i}^{+}} \bar{r}_{jk}^{\mathbf{P}}x_{jk}^{\mathbf{P}}(t)\right) + \sum_{i \in \mathcal{A}_{i}} \sum_{j \in \Gamma^{+}} \mathbb{E}\left[d_{i}^{\mathbf{P}}(t)\bar{r}_{ij}^{\mathbf{P}}x_{ij}^{\mathbf{P}}(t) \middle|\mathbf{x}^{\mathbf{P}}(t)\right]$$

$$(44)$$

Then we obtain

$$\mathbb{E}\left[\mathbf{x}^{\mathbf{P}}(t)^{\mathrm{T}}\boldsymbol{\delta}(t)|\mathbf{x}^{\mathbf{P}}(t)\right] = \sum_{i \in \mathcal{A}_{i} \cup \mathcal{A}_{e}} \mathbb{E}\left[\min\left\{Q_{ij}^{\mathbf{P}}s_{ij}(t), x_{ij}^{\mathbf{P}}(t)\right\} \left|\mathbf{x}^{\mathbf{P}}(t)\right] \times \left(-x_{ij}^{\mathbf{P}}(t) + \sum_{k \in I_{i}^{+}} \bar{r}_{jk}^{\mathbf{P}}x_{jk}^{\mathbf{P}}(t)\right) + \sum_{i \in \mathcal{A}_{r}} \bar{d}_{i}^{\mathbf{P}} \bar{r}_{ji}^{\mathbf{P}}x_{ij}^{\mathbf{P}}(t)\right]$$

$$(45)$$

For the last term of Eq. (45), $\sum_{i \in A_e} \bar{d}_i^P \bar{r}_{ij}^P x_{ij}^P(t)$, we have

$$\sum_{i \in \mathcal{A}_{e}} \bar{d}_{i}^{P} \bar{r}_{ij}^{P} x_{ij}^{P}(t) = \sum_{i \in \mathcal{A}_{e}} f_{ij}^{P} \bar{r}_{ij}^{P} x_{ij}^{P}(t) = \sum_{i \in \mathcal{A}_{e}} f_{ij}^{P} x_{ij}^{P}(t)$$
 (46)

$$= \sum_{i \in \mathcal{A}_i \cup \mathcal{A}_n} f_i^P \bar{r}_{ij}^P x_{ij}^P(t) - \sum_{i \in \mathcal{A}_i} f_j^P \bar{r}_{jk}^P x_{jk}^P(t)$$

$$\tag{47}$$

$$= \sum_{i \in \mathcal{A}_i \cup \mathcal{A}_c} f_i^P \bar{r}_{ij}^P x_{ij}^P(t) - \sum_{j \in \Gamma_i^+} \left[\sum_{i \in \mathcal{A}_i \cup \mathcal{A}_c} f_i^P \bar{r}_{ij}^P \right] \sum_{k \in \Gamma_i^+} \bar{r}_{jk}^P x_{jk}^P(t)$$

$$(48)$$

$$= \sum_{i \in \mathcal{A}_i \cup \mathcal{A}_c} f_i^P \bar{r}_{ij}^P \left(x_{ij}^P(t) - \sum_{k \in \mathcal{L}^+} \bar{r}_{jk}^P x_{jk}^P(t) \right)$$
 (49)

By Proposition 1 there exists some $\bar{s}_{ij} \in \text{Conv}(S_p)$ such that $\mathbb{E}[s_{ij}(t)] = \bar{s}_{ij}$. Then

$$\mathbb{E}\left[\mathbf{x}^{\mathbf{P}}(t)^{\mathsf{T}}\boldsymbol{\delta}(t)|\mathbf{x}^{\mathbf{P}}(t)\right] = \sum_{i \in \mathcal{A}_{i} \cup \mathcal{A}_{c}} \left(f_{i}^{\mathbf{P}} \bar{r}_{ij}^{\mathbf{P}} - \mathbb{E}\left[\min\left\{Q_{ij}^{\mathbf{P}} s_{ij}(t), \mathbf{x}^{\mathbf{P}}(t)\right\} \middle| \mathbf{x}^{\mathbf{P}}(t)\right]\right) \left(x_{ij}^{\mathbf{P}}(t) - \sum_{k \in \Gamma_{j}^{+}} \bar{r}_{jk}^{\mathbf{P}} x_{jk}^{\mathbf{P}}(t)\right)$$

$$= \sum_{i \in \mathcal{A}_{i} \cup \mathcal{A}_{c}} \left(f_{i}^{\mathbf{P}} \bar{r}_{ij}^{\mathbf{P}} - \bar{s}_{ij} Q_{ij}^{\mathbf{P}}\right) \left(x_{ij}^{\mathbf{P}}(t) - \sum_{k \in \Gamma_{j}^{+}} \bar{r}_{jk}^{\mathbf{P}} x_{jk}^{\mathbf{P}}(t)\right)$$

$$+ \sum_{i \in \mathcal{A}_{i} \cup \mathcal{A}_{c}} \left(\bar{s}_{ij} Q_{ij}^{\mathbf{P}} - \mathbb{E}\left[\min\left\{Q_{ij}^{\mathbf{P}} s_{ij}(t), x_{ij}^{\mathbf{P}}(t)\right\} \middle| \mathbf{x}^{\mathbf{P}}(t)\right]\right)$$

$$\times \left(x_{ij}^{\mathbf{P}}(t) - \sum_{k \in \Gamma^{+}} \bar{r}_{jk}^{\mathbf{P}} x_{jk}^{\mathbf{P}}(t)\right)$$

$$(51)$$

For the second term of Eq. (51), if $x_{ij}^{\mathrm{P}}(t) \geq Q_{ij}^{\mathrm{P}}$, then we have $\mathbb{E}\left[\min\left\{Q_{ij}^{\mathrm{P}}s_{ij}(t), x_{ij}^{\mathrm{P}}(t)\right\} \middle| \mathbf{x}^{\mathrm{P}}(t)\right] = Q_{ij}^{\mathrm{P}}\bar{s}_{ij}$. Therefore, the second term of Eq. (51) equals zero. If $x_{ij}^{\mathrm{P}}(t) < Q_{ij}^{\mathrm{P}}$, then we have $\mathbb{E}\left[\min\left\{Q_{ij}^{\mathrm{P}}s_{ij}(t), x_{ij}^{\mathrm{P}}(t)\right\} \middle| \mathbf{x}^{\mathrm{P}}(t)\right] = \mathbb{E}\left[x_{ij}^{\mathrm{P}}(t)\middle| \mathbf{x}^{\mathrm{P}}(t)\right]$, which results in

$$\sum_{i \in \mathcal{A}_{i} \cup \mathcal{A}_{e}} \left(\bar{s}_{ij} Q_{ij}^{P} - \mathbb{E} \left[x_{ij}^{P}(t) \middle| \mathbf{x}^{P}(t) \right] \right) \left(x_{ij}^{P}(t) - \sum_{k \in \Gamma_{j}^{+}} \bar{r}_{jk}^{P} x_{jk}^{P}(t) \right) \leq \sum_{i \in \mathcal{A}_{i} \cup \mathcal{A}_{e}} \bar{s}_{ij} Q_{ij}^{P} x_{ij}^{P}(t)$$

$$\leq \sum_{i \in \mathcal{A}_{i} \cup \mathcal{A}_{e}} \left(Q_{ij}^{P} \right)^{2}$$

$$(52)$$

Therefore, the second term of Eq. (51) is equal to zero or bounded by $\sum_{i \in \mathcal{A}_i \cup \mathcal{A}_e} \left(Q_{ij}^P\right)^2$. Moving on, we focus on the first term of Eq. (51). Based on inequality (28), we have

$$\sum_{i \in \mathcal{A}_i \cup \mathcal{A}_e} \left(f_i^P \bar{r}_{ij}^P - \bar{s}_{ij} Q_{ij}^P \right) \left(x_{ij}^P (t) - \sum_{k \in \Gamma_j^+} \bar{r}_{jk}^P x_{jk}^P (t) \right) \le \sum_{i \in \mathcal{A}_i \cup \mathcal{A}_e} \left(f_i^P \bar{r}_{ij}^P - \bar{s}_{ij} Q_{ij}^P \right) \left(x_{ij}^P (t) \right)$$

$$\le -\epsilon |\mathbf{x}^P (t)|$$

$$(53)$$

Eq. (37) satisfies the following relationship based on Eqs. (52) and (53):

$$\left|\delta_{ij}(t)\right| = \left|-\min\left\{Q_{ij}^{\mathbf{P}}s_{ij}(t), x_{ij}^{\mathbf{P}}(t)\right\} + \sum_{h \in \mathcal{A}_{-}^{-}}\min\left\{Q_{hi}^{\mathbf{P}}s_{ij}(t), x_{hi}^{\mathbf{P}}(t)\right\} \times r_{ij}^{\mathbf{P}}(t)\right| \quad \forall i \in \mathcal{A}_{i}, j \in \Gamma_{i}^{+}$$

$$(54)$$

$$\leq \max \left\{ Q_{ij}^{\mathrm{P}}, \sum_{h \in \mathcal{A}_{i}^{-}} Q_{ij}^{\mathrm{P}} \right\} \tag{55}$$

Let \hat{d}_{ij} be the maximum value of the demand. Then we have

$$\left|\delta_{ij}(t)\right| = \left|-\min\left\{Q_{ij}^{\mathrm{P}}s_{ij}(t), x_{ij}^{\mathrm{P}}(t)\right\} + d_{i}^{\mathrm{P}}(t) \times r_{ij}^{\mathrm{P}}\right| \le \max\left\{Q_{ij}^{\mathrm{P}}, \hat{d}_{ij}\right\} \quad \forall i \in \mathcal{A}_{\mathrm{e}}, j \in \Gamma_{i}^{+}$$

$$(56)$$

Define λ as the maximum value among Q_{ij}^P , $\sum_{h \in \mathcal{A}_i^-} Q_{ij}^P$, and \hat{d}_{ij} , that is

$$\lambda = \max \left\{ Q_{ij}^{P}, \sum_{h \in \mathcal{A}_{i}^{-}} Q_{ij}^{P}, \hat{d}_{ij} \right\}$$
 (57)

Because the total movement of private vehicles is M, we have the following inequality

$$\left|\delta_{ij}(t)\right|^2 \le M \times \lambda^2 \tag{58}$$

From Eqs. (53) and (58)

$$\left|\mathbf{x}^{\mathbf{P}}(t+1)\right|^{2} - \left|\mathbf{x}^{\mathbf{P}}(t)\right|^{2} = 2\mathbf{x}^{\mathbf{P}}(t)^{\mathrm{T}}\boldsymbol{\delta} + \left|\boldsymbol{\delta}\right|^{2}$$

$$\leq 2\left(\sum_{i \in \mathcal{A}_{i} \cup \mathcal{A}_{e}} (Q_{ij}^{\mathbf{P}})^{2} - \epsilon |\mathbf{x}^{\mathbf{P}}(t)|\right) + M\lambda^{2}$$
(59)

$$=\kappa - \epsilon |\mathbf{x}^{\mathbf{P}}(t)| \tag{60}$$

where $\kappa = 2 \sum_{i \in A_i \cup A_e} (Q_{ii}^P)^2 + M \lambda^2$.

Based on the above procedure, we find that we do not need to know the lower-bound and upper-bound of signal to prove stability. What we need is the long-time average time \bar{s}_{ij} used for serving turning movement (i,j) while considering transit signal priority.

Proposition 3. When average signal \bar{s}_{ij} , which satisfies the stable region constrains and obey the transit signal priority, is used and $\bar{d}^P \in \mathcal{D}^0$, the transportation network is stable.

Proof. Inequality (37) holds from Lemma 1. Taking expectations and summing over t = 1, ..., T gives the following inequality:

$$\mathbb{E}\left[\nu(T+1) - \nu(1)|\mathbf{x}^{P}(t)\right] \le \kappa T - \epsilon \sum_{t=1}^{T} |\mathbf{x}^{P}(t)| \tag{61}$$

Then we have

$$\epsilon \frac{1}{T} \sum_{t=1}^{T} \mathbb{E}\left[|\mathbf{x}^{\mathbf{P}}(t)| \right] \le \kappa - \frac{1}{T} \mathbb{E}\left[\nu(T+1) \right] + \frac{1}{T} \mathbb{E}\left[\nu(1) \right] \le \kappa + \frac{1}{T} \mathbb{E}\left[\nu(1) \right]$$
(62)

Table 1 Notation.	
M	Set of movements
N	Set of nodes
${\cal A} \ \Gamma_j^+$	Set of links Set of outgoing links
Γ_j^-	Set of incoming links
$x_{ij}^{\mathrm{P}}(t)$	Number of private vehicles of the movement from link i to link j at time step t
$x_{ij}^{\mathrm{B}}(t)$	Number of buses of the movement from link i to link j at time step t
$r_{ij}^{\rm P}(t)$	Proportion of private vehicles entering i that will next move to j .
$r_{ij}^{\mathrm{B}}(t)$	Proportion of buses entering i that will next move to j .
$w_{ij}^{\rm P}(t)$	Weight of turning movement from link i to link j at time step t
$d_i^{\rm B}(t)$	Bus demand at link i
$d_i^{\rm P}(t)$	Private vehicle demand at link i
$s_{ij}(t)$	Actuation of turning movement from link i to link j at time step t
$y_{ij}^{\mathbf{p}}(t)$	Signal control private vehicle flow from link i to link j at time step t
$y_{ij}^{\rm B}(t)$	Signal control number of buses from link i to link j at time step t
$Q_{ij}^{ m P}$	Capacity of turning movement for private vehicles from link i to link j
$Q_{ij}^{ m B}$	Capacity of turning movement for buses from link i to link j
Q_c	Capacity of conflict region
α_{ij}^n	0–1 binary dummy variable $(\alpha_{ij}^n = 1$ when private vehicles have conflict with buses)
f_i^{P}	Average private vehicle traffic volume of link i.

which immediately implies that the stability Definition 1 is satisfied. \Box

Furthermore, we can prove that stability is not impacted by the initial condition. For Eq. (62), we move ϵ to the right hand side and take the limit as T goes to infinity. Then the $\frac{1}{T}\mathbb{E}[v(1)]$ term equals zero, which yields

$$\lim_{T \to \infty} \frac{1}{T} \sum_{t=0}^{T} \mathbb{E}\left[|\mathbf{x}^{P}(t)| \right] \le \frac{\kappa}{\epsilon}$$
 (63)

4. Modified max-pressure control policy

4.1. Notations

See Table 1.

4.2. Max-pressure control policy considering public transit signal priority

This study uses the max-pressure control policy to calculate how many vehicles at the intersection should be served at every time step integrated the transit signal priority. The weight of each turning movement is the queue length of this movement (i, j) of private vehicles. The pressure calculation is shown by Eq. (64). As shown in Fig. 1, the downstream turning movements of movement (i, j) are composed by movement (j, k_1) , (j, k_2) , and (j, k_3) .

$$w_{ij}^{P}(t) = x_{ij}^{P}(t) - \sum_{k \in \Gamma_{jk}^{+}} r_{jk}^{P}(t) x_{jk}^{P}(t)$$
(64)

After we calculate the weight for each movement, a mixed-integer linear program is used to calculate the intersection control. In this program, we use a_{ij}^n we indicate whether the buses' movements have conflicts with private vehicles. The capacity of conflict region is Q_c , which is determined by the capacities of turning movements, $Q_c = \max_{(i,j)|c \in C_{ij}} \{Q_{ij}\}$. The total number of private vehicles and buses driving through the one conflict region per time is bounded by the capacity of the conflict region.

The max-pressure control policy considering bus priority tries to maximize the total pressure of private vehicles. Let $s_{ij}^*(t)$ denote the max-pressure signal control at intersection n in the transportation network given the priority of bus transit, which is $s_{ij}^*(t) = \operatorname{argmax}_{s \in S_p} \left[\sum_{(i,j) \in \mathcal{M}} s_{ij}(t) Q_{ij}^p w_{ij}^p(t) \right]$ based on constraints (65b) to (65h). To be specific, constraint (65b) is combined with Eq. (11) that indicates the max-pressure control gives priority to the bus transit. Specifically, once a bus appears in the area of the intersection, our signal control $s_{ij}(t)$ will be activated ($s_{ij}(t) = 1$) in this moving direction. However, if there is no bus, $s_{ij}(t)$ is controlled by the pressure of private vehicles, which is determined by the objective function, Eq. (65a). If two buses with conflicting movements are waiting, then one of them will be given a green light. The optimal solution to problem (65a) determines which bus will move first. The operation of transit signal priority is described in Fig. 3. Private vehicles would follow the bus transit priority

signal. Constraint (65c) indicated the movement of private vehicles should consider the capacity of this movement and whether this movement could conflict with buses or not. Constraint (65d) indicates the sum movements of private vehicles and buses should less equal to the capacity of the conflict region. Constraint (65e) indicates the movement of private vehicles should be less than or equal to the queue length of the private vehicles. Constraint (65f) indicates the bus movement flow is bounded by the minimum value of capacity multiples signal control or the length of bus queueing. (65g) means the signal control equal to 0 or 1. The constraint (65h) indicates the queueing length of buses, the movement of private vehicles and buses should not be negative numbers.

$$\sum_{(i,j)\in\mathcal{M}} s_{ij}(t)Q_{ij}^{P}w_{ij}^{P}(t)$$
(65a)

s.t.
$$\sum_{(i,j)\in\mathcal{M}} x_{ij}^{\mathsf{B}}(t) \left[\sum_{(i,j)\in\mathcal{M}} s_{ij}(t) x_{ij}^{\mathsf{B}}(t) - 1 \right] \ge 0 \qquad \forall (i,j)\in\mathcal{M}$$
 (65b)

$$y_{ii}^{\mathbf{P}}(t) \le s_{ii}(t)Q_{ii}^{\mathbf{P}}(1 - \alpha_{ii}^{n}) \qquad \qquad \forall (i, j) \in \mathcal{M}$$
 (65c)

$$\sum_{(i, j) \in \mathcal{M}} y_{ij}^{\mathbf{P}}(t)(1 - \alpha_{ij}^n) + y_{ij}^{\mathbf{B}}(t) \le Q_{\mathbf{c}}$$
 $\forall (i, j) \in \mathcal{M}, \forall c \in \mathcal{C}$ (65d)

$$y_{ii}^{P}(t) \le x_{ii}^{P}(t)$$
 $\forall (i,j) \in \mathcal{M}$ (65e)

$$y_{ij}^{\mathrm{B}}(t) = \min \left\{ Q_{ij}^{\mathrm{B}} s_{ij}(t), x_{ij}^{\mathrm{B}}(t) \right\} \qquad \forall (i, j) \in \mathcal{M}$$
 (65f)

$$s_{ij}(t) \forall \in \{0, 1\}$$
 $\forall (i, j) \in \mathcal{M}$ (65g)

$$x_{ij}^{\mathrm{B}}(t), y_{ij}^{\mathrm{P}}(t), y_{ij}^{\mathrm{B}}(t) \ge 0 \qquad \qquad \forall (i,j) \in \mathcal{M}$$
 (65h)

Lemma 2. If max-pressure control policy considering bus priority is used and $\bar{\mathbf{d}}^P \in \mathcal{D}^0$, then we have the following inequality for \bar{s}_{ij} , which is the average signal control considering bus priority and satisfying constraints (25)–(27).

$$\mathbb{E}\left[\sum_{(i,j)\in\mathcal{M}^2} s_{ij}^{\star}(t)Q_{ij}^{\mathbf{p}}w_{ij}^{\mathbf{p}}(t) \left| \mathbf{x}^{\mathbf{p}}(t) \right| \mathbf{x}^{\mathbf{p}}(t)\right] \ge \mathbb{E}\left[\sum_{(i,j)\in\mathcal{M}^2} \bar{s}_{ij}Q_{ij}^{\mathbf{p}}w_{ij}^{\mathbf{p}}(t) \left| \mathbf{x}^{\mathbf{p}}(t) \right| \right]$$
(66)

Proof. First, we have

$$\sum_{(i,j)\in\mathcal{M}^2} s_{ij}^{\star}(t) Q_{ij}^{P} w_{ij}^{P}(t) \ge \sum_{(i,j)\in\mathcal{M}^2} s_{ij}(t) Q_{ij}^{P} w_{ij}^{P}(t)$$
(67)

since $s_{ij}^{\star}(t)$, $s_{ij}(t) \in S_p$, and $s_{ij}^{\star}(t)$ maximizes objective (65a). Then we calculate the expected value of the above equation when given the private vehicle queue length $\mathbf{x}^{\mathrm{P}}(t)$ as

$$\mathbb{E}\left[\sum_{(i,j)\in\mathcal{M}^2} s_{ij}^{\star}(t)Q_{ij}^{\mathbf{p}}w_{ij}^{\mathbf{p}}(t)\middle|\mathbf{x}^{\mathbf{p}}(t)\middle|\mathbf{x}^{\mathbf{p}}(t)\right] \ge \mathbb{E}\left[\sum_{(i,j)\in\mathcal{M}^2} s_{ij}(t)Q_{ij}^{\mathbf{p}}w_{ij}^{\mathbf{p}}(t)\middle|\mathbf{x}^{\mathbf{p}}(t)\right]$$

$$\tag{68}$$

Since $s_{ij}^{\star}(t) = \operatorname{argmax}_{s \in S} \sum_{(i,j) \in \mathcal{M}^2} s_{ij}(t) Q_{ij}^{P} w_{ij}^{P}(t)$ and based on Eq. (12), we rewrite Eq. (68) to

$$\mathbb{E}\left[\sum_{(i,j)\in\mathcal{M}^2} s_{ij}^{\star}(t)Q_{ij}^{P}w_{ij}^{P}(t) \left| \mathbf{x}^{P}(t) \right| \ge \mathbb{E}\left[\sum_{(i,j)\in\mathcal{M}^2} \bar{s}_{ij}Q_{ij}^{P}w_{ij}^{P}(t) \left| \mathbf{x}^{P}(t) \right| \right] \quad \Box$$
(69)

4.3. Stability analysis

Now, we proceed to prove that the max-pressure signal control with bus priority defined in 4 will stabilize any private vehicle demand $\bar{\mathbf{d}}^P \in \mathcal{D}^0$. Notice that the bus demand can be stabilized at any time since the number of buses is limited and much smaller than the number of private vehicles.

Lemma 3. If max-pressure signal control with bus priority is used and $\bar{\mathbf{d}}^P \in \mathcal{D}^0$, there exists a Lyapunov function $v(t) \geq 0$ and constants $\kappa > 0$, $\epsilon > 0$ such that

$$\mathbb{E}\left[\left|v(t+1) - v(t)\right| \mathbf{x}^{\mathbf{P}}(t)\right] \le \kappa - \eta |\mathbf{x}^{\mathbf{P}}(t)| \tag{70}$$

Proof. Based on Eqs. (7)-(44) and the definition of the pressure term (64), we obtain

$$\mathbb{E}\left[\mathbf{x}^{\mathbf{P}}(t)^{\mathsf{T}}\boldsymbol{\delta}(t)|\mathbf{x}^{\mathbf{P}}(t)\right] = \sum_{i \in \mathcal{A}_{i} \cup \mathcal{A}_{c}} \mathbb{E}\left[\min\left\{Q_{ij}^{\mathbf{P}}s_{ij}(t), x_{ij}^{\mathbf{P}}(t)\right\} \middle| \mathbf{x}^{\mathbf{P}}(t)\right] \times \left(-w_{ij}^{\mathbf{P}}(t)\right) + \sum_{i \in \mathcal{A}_{c}} \bar{d}_{i}^{\mathbf{P}} \bar{r}_{ij}^{\mathbf{P}} x_{ij}^{\mathbf{P}}(t)$$
(71)

The last term of Eq. (71) can be rewritten as follows based on Eqs. (25), (26), and (64):

$$\sum_{i \in A} d_i^p \bar{r}_{ij}^p x_{ij}^p(t) = \sum_{i \in A} f_{ij}^p x_{ij}^p(t)$$
 (72)

$$= \sum_{i \in A_{a} \cup A_{a}} f_{i}^{P} \bar{r}_{ij}^{P} x_{ij}^{P}(t) - \sum_{i \in A_{i}} f_{j}^{P} \bar{r}_{jk}^{P} x_{jk}^{P}(t)$$
 (73)

$$= \sum_{i \in \mathcal{A}_{e} \cup \mathcal{A}_{e}} f_{i}^{P} \bar{r}_{ij}^{P} x_{ij}^{P}(t) - \sum_{j \in \Gamma_{i}^{+}} \left(f_{i}^{P} \bar{r}_{ij}^{P} \right) \sum_{k \in \Gamma_{i}^{+}} \bar{r}_{jk}^{P} x_{jk}^{P}(t) \tag{74}$$

$$= \sum_{i \in \mathcal{A}_i \cup \mathcal{A}_i} f_i^{\mathsf{P}} \bar{r}_{ij}^{\mathsf{P}} \left(w_{ij}^{\mathsf{P}}(t) \right) \tag{75}$$

Combining Eqs. (71) and (75) yields

$$\mathbb{E}\left[\mathbf{x}^{P}(t)^{T}\boldsymbol{\delta}(t)|\mathbf{x}^{P}(t)\right] = \sum_{i \in \mathcal{A}_{i} \cup \mathcal{A}_{e}} \left(f_{i}^{P}\bar{r}_{ij}^{P} - \mathbb{E}\left[\min\left\{Q_{ij}^{P}s_{ij}(t), x_{ij}^{P}(t)\right\} \middle| \mathbf{x}^{P}(t)\right]\right) w_{ij}^{P}(t)$$

$$= \sum_{i \in \mathcal{A}_{i} \cup \mathcal{A}_{e}} \left(f_{i}^{P}\bar{r}_{ij}^{P} - Q_{ij}^{P}\bar{s}_{ij}\right) w_{ij}^{P}(t)$$

$$(76)$$

$$+ \sum_{i \in \mathcal{A}_i \cup \mathcal{A}_c} \left(Q_{ij}^{P} \bar{s}_{ij} - \mathbb{E} \left[\min \left\{ Q_{ij}^{P} s_{ij}(t), x_{ij}^{P}(t) \right\} \middle| \mathbf{x}^{P}(t) \right] \right) w_{ij}^{P}(t)$$

$$(77)$$

For the second term of Eq. (77), if $x_{ij}^{P}(t) \geq Q_{ij}^{P}$, then we have $\mathbb{E}\left[\min\left\{Q_{ij}^{P}s_{ij}(t), x_{ij}^{P}(t)\right\} \middle| \mathbf{x}^{P}(t)\right] = Q_{ij}^{P}\bar{s}_{ij}$. Therefore, the second term of Eq. (77) equals zero. If $x_{ij}^{\mathrm{P}}(t) < Q_{ij}^{\mathrm{P}}$, then we have $\mathbb{E}\left[\min\left\{Q_{ij}^{\mathrm{P}}s_{ij}(t),x_{ij}^{\mathrm{P}}(t)\right\}\left|\mathbf{x}^{\mathrm{P}}(t)\right|\right] = \mathbb{E}\left[x_{ij}^{\mathrm{P}}(t)\left|\mathbf{x}^{\mathrm{P}}(t)\right|\right]$. Therefore, we obtain the following

$$\left(Q_{ij}^{\mathbf{P}}\bar{s}_{ij} - \mathbb{E}\left[x_{ij}^{\mathbf{P}}(t)\middle|\mathbf{x}^{\mathbf{P}}(t)\right]\right)w_{ij}^{\mathbf{P}}(t) \le Q_{ij}^{\mathbf{P}}x_{ij}^{\mathbf{P}}(t) \le \left(Q_{ij}^{\mathbf{P}}\right)^{2} \tag{78}$$

Hence, the second term of Eq. (77) equals zero or is bounded by $\sum_{i \in A_i \cup A_e} \left(Q_{ij}^P \right)^2$. The max-pressure signal control $s_{ij}^{\star}(t)$ is chosen from the feasible signal control set S_p , which obeys bus priority constraints, and $s_{i}^{\star}(t)$ seeks to maximize the objective (65a). According to Lemma 2, we have

$$\mathbb{E}\left[\sum_{i \in \mathcal{A}_i \cup \mathcal{A}_c} \left(f_i^P \bar{r}_{ij}^P - s_{ij}^{\star}(t) Q_{ij}^P\right) w_{ij}^P(t) \middle| w_{ij}^P(t) \middle| w_{ij}^P(t) \right] \le \mathbb{E}\left[\sum_{i \in \mathcal{A}_i \cup \mathcal{A}_c} \left(f_i^P \bar{r}_{ij}^P - \bar{s}_{ij} Q_{ij}^P\right) w_{ij}^P(t) \middle| w_$$

Therefore, for some feasible signal controls $s_{ij}(t)$ satisfying the stable region and integrated transit signal priority, we obtain \bar{s}_{ij} based on Eq. (12). We have

$$\sum_{i \in \mathcal{A}_i \cup \mathcal{A}_e} \left(f_i^P \bar{r}_{ij}^P - \bar{s}_{ij} Q_{ij}^P \right) w_{ij}^P(t) \le -\epsilon \sum_{(i,j) \in \mathcal{M}^2} \max \left\{ w_{ij}^P, 0 \right\} \le -\epsilon |w_{ij}^P|$$

$$\tag{80}$$

We know that the pressure $\mathbf{w}(t)$ is a linear function of the queue length of the private vehicles. So we can find $\beta > 0$ to satisfy $\sum_{(i,j)\in\mathcal{M}^2} w_{ij}^P \geq \beta |\mathbf{x}^P|$. Then we have

$$-\epsilon |w_{ij}^{P}| \le -\epsilon \beta |\mathbf{x}^{P}| \le \sum_{i \in A \cup A} \left(Q_{ij}^{P} \right)^{2} - \epsilon \beta |\mathbf{x}^{P}| \tag{81}$$

 $\delta_{ij}(t)$ is upper-bounded by $\max\left\{Q_{ij}^{\mathrm{P}}, \sum_{h \in \mathcal{A}_{i}^{-}} Q_{ij}^{\mathrm{P}}\right\}$, which is the same as Eq. (54). Based on Eq. (81) and Eqs. (54)–(58), we obtain

$$\left|\mathbf{x}^{\mathbf{P}}(t+1)\right|^{2} - \left|\mathbf{x}^{\mathbf{P}}(t)\right|^{2} = 2\mathbf{x}^{\mathbf{P}}(t)^{\mathsf{T}}\boldsymbol{\delta} + \left|\boldsymbol{\delta}\right|^{2}$$

$$\leq 2\left(\sum_{i \in \mathcal{A}_{i} \cup \mathcal{A}_{e}} \left(Q_{ij}^{\mathbf{P}}\right)^{2} - \epsilon \beta |\mathbf{x}^{\mathbf{P}}(t)|\right) + M\lambda^{2}$$
(82)

$$= \kappa - \eta |\mathbf{x}^{\mathsf{P}}(t)| \tag{83}$$

where $\kappa = 2 \sum_{i \in A_i \cup A_n} (Q_{ii}^P)^2 + M \lambda^2$, $\epsilon \beta = \lambda$.

Proposition 4. When $\bar{\mathbf{d}}^{\mathrm{P}} \in \mathcal{D}^{0}$, then the max-pressure policy considering transit signal priority is stabilizing.

Proof. The proof is analogous to Proposition 3. Inequality (70) holds from Lemma 3. Taking expectations, summing over t = 1, ..., T, and transferring the position of terms gives the following inequality:

$$\eta \frac{1}{T} \sum_{t=1}^{T} \mathbb{E}\left[|\mathbf{x}^{\mathsf{P}}(t)| \right] \le \kappa - \frac{1}{T} \mathbb{E}\left[\nu(T+1) \right] + \frac{1}{T} \mathbb{E}\left[\nu(1) \right] \le \kappa + \frac{1}{T} \mathbb{E}\left[\nu(1) \right]$$
(84)

which satisfies Definition 1 for stability.

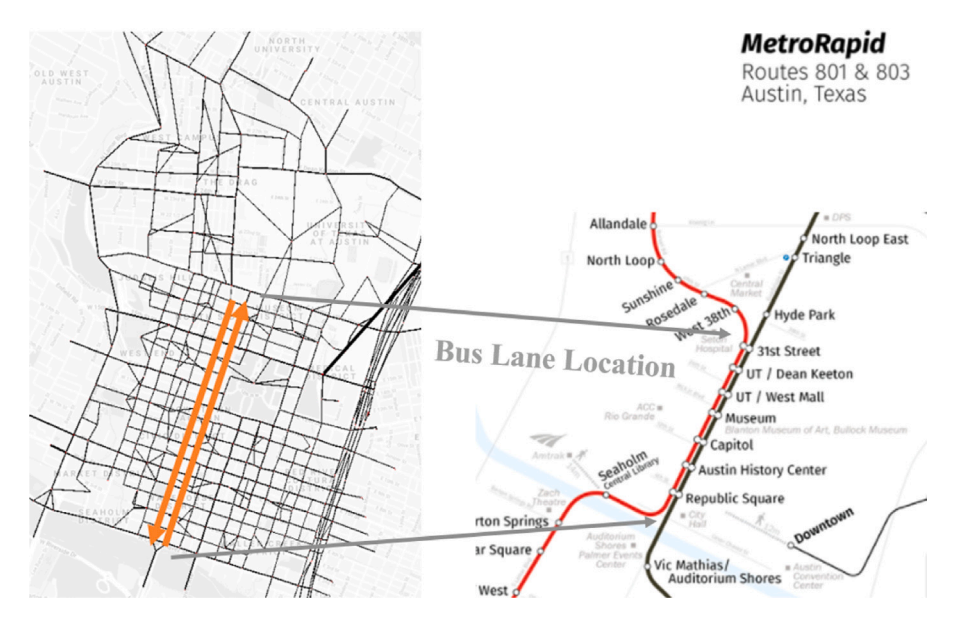


Fig. 4. Austin network with bus lanes.

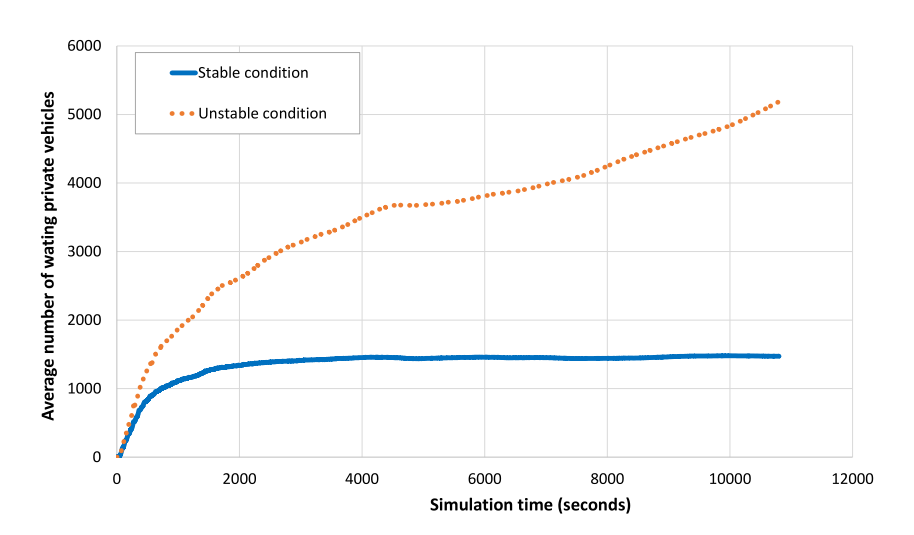


Fig. 5. An example of stable and unstable region.

5. Simulation model and numerical results

To test the effects of our proposed max-pressure control policy, we set up simulations on the downtown Austin Network based on a microscopic traffic simulation tool, SUMO, interfaced with Python (Lopez et al., 2018). The demand file was from the authors' past study, which can be found on Levin et al. (2020). Note that, there are two bus lanes built in the downtown area, the Austin Metro Rapid, which is the bus rapid transit. Details are shown in Fig. 4. We add the Metro Rapid information into the simulation settings, such as bus operational timetable and departure interval of routes and to make the simulation much closer to the real-world condition. All the bus operational information is open access to the public on the Capital Metro website.

The numerical results presented in this part compare the performance of the max-pressure control considering transit signal priority of bus rapid transit system (referred to as MP-TSP), adaptive signal control considering transit signal priority (referred to as Adaptive-TSP), and a given fixed-time controller (referred to as FT-TSP) considering transit signal priority of bus rapid transit system. It is worth noticing that we only give transit signal priority to built-in bus lanes. While, when there is no bus lane on a BRT route, transit signal priority will fail for any signal controller in this simulation. In this simulation, there is no conflicting movement for bus lanes in the Austin network, and the transit signal priority strategy is the same for all traffic signal control policies in this paper.

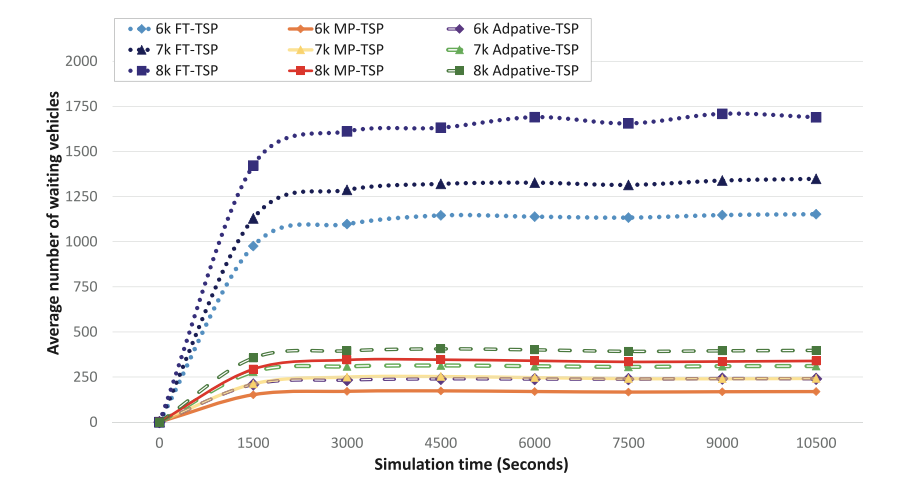


Fig. 6. Network stability.

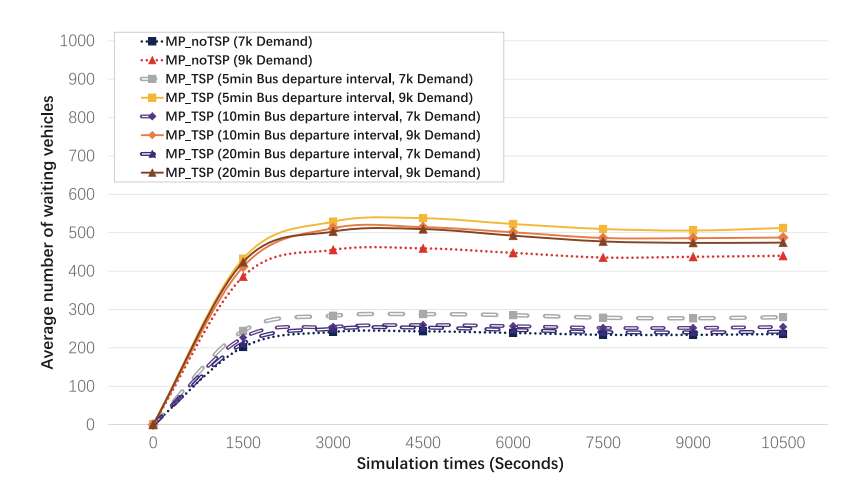


Fig. 7. Stable region comparison between MP-noTSP and MP-TSP.

5.1. Stability comparison

First, we compare the stability of the network based on Definition 1. Basically, we test whether the total number of private vehicles in the network is increasing over time under different private vehicle demand level settings with 20 min bus departure intervals. Fig. 5 shows an example of a stable condition and unstable condition. When the demand of private vehicles is within the stable region, the average number of private vehicles will converge to a constant. However, for unstable demand, the average number of private vehicles will increase to an arbitrarily large number.

Fig. 6 compares the result of the average number of waiting private vehicles for FT-TSP, Adaptive-TSP, and MP-TSP. At the same private vehicles' demand setting, the number of waiting private vehicles by FT-TSP and Adaptive-TSP are larger than the results for MP-TSP. Furthermore, when increasing the demand level, the MP-TSP has a lower number of waiting private vehicles. These results indicate that MP-TSP has a larger stable region than FT-TSP and Adaptive-TSP, and is able to stabilize the network at a higher level of private vehicle demand, which is consistent with Section 4.2.

It is also worth exploring whether the signal priority affects the stable region. We compare the original max pressure control (referred to as MP-noTSP) from Varaiya (2013) with MP-TSP under different bus departure intervals. The results are shown in Fig. 7. These results show that when the number of waiting private vehicles of MP-noTSP is lowest under the same demand setting. This is because, if we give more priority to transit, we will sacrifice the right of way at the intersection for private vehicles. When the bus arrival frequency is higher (bus departure interval is smaller), the number of waiting private vehicles of MP-TSP is higher. This is reasonable because the higher the bus demand, the more priority time buses are given.

From Fig. 7, we find that TSP may "reduce" the stable region of private vehicles. Specifically, the original private vehicle demand may be within the stable region, but when TSP is considered, the private vehicle demand may fall outside of the stable region.

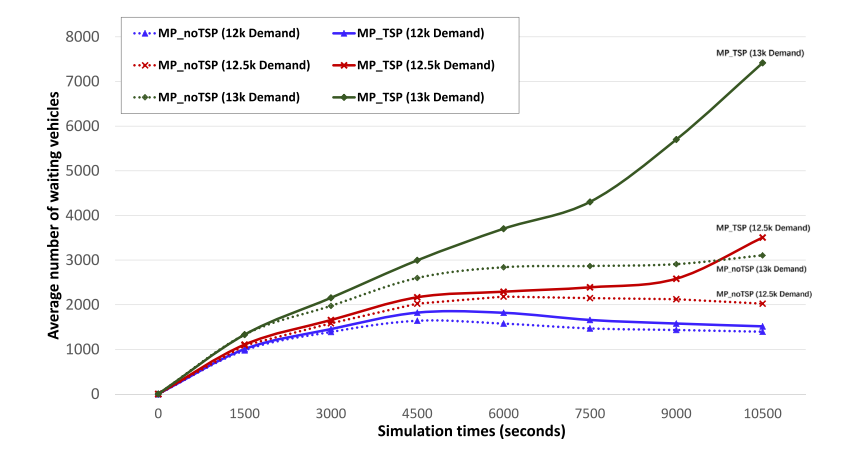
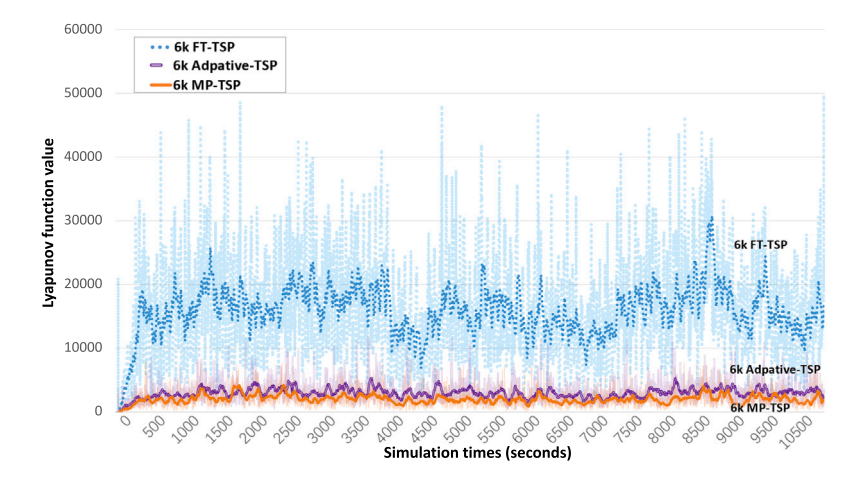


Fig. 8. Impacts of TSP on original stable demand.



 $\textbf{Fig. 9.} \ \ \textbf{Trajectory of Lyapunov function under demand of } 6000 \ \ \textbf{vehicles per hour}.$

Fig. 8 shows the detail of throughput loss in experiments under 20 min bus departure intervals setting. Fig. 8 shows that when we choose MP-noTSP, the network can serve 12500 private vehicles per hour, while when implementing MP-TSP, the network becomes unstable (the average number of waiting vehicles increases to infinity). When we add private vehicle demand to 13000 vehicles per hour, both MP-noTSP and MP-TSP cannot stabilize the network. It is worth noticing when implementing MP-TSP, the network can serve 12000 private vehicles per hour. Therefore, we may lose around 500 private vehicles network capacity when giving signal priority to public transit.

We also provide the trajectory of the proposed Lyapunov function (40) as figures to show the dynamic pattern of stability for FT-TSP, Adaptive-TSP, and MP-TSP. The demand setting and bus departure interval setting is the same as in Fig. 5. As Figs. 9–11 show, the Lyapunov function value of MP-TSP is still the lowest compared with Adaptive-TSP and FT-TSP. These results indicate that MP-TSP has a larger potential to achieve maximum stability on a given network under different levels of demand.

5.2. Travel time

It is also important to explore how transit signal priority impacts vehicle travel time at the network level. The average waiting time of MP-TSP, Adaptive-TSP, and FT-TSP at different demand levels and 20 min bus departure intervals time are shown in Fig. 12. We also provide Table 2 including experiment results for better comparison. As the demand increases, vehicles spend more time on the links and intersections. Therefore, the average waiting time increases. Unsurprisingly, since MP-TSP can serve more demand than Adaptive-TSP and FT-TSP, MP-TSP have lower average travel time compared with adaptive-TSP and FT-TSP. Also, it is no surprise that Adaptive-TSP make private vehicles have less travel time than FT-TSP controller since it could adjust phases duration based on loop detectors. These results also indicate that the max-pressure controller integrated with transit signal priority performs

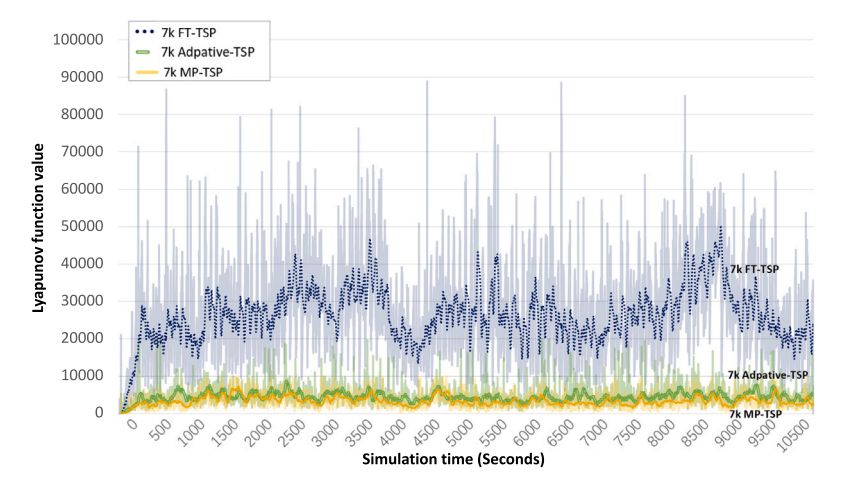


Fig. 10. Trajectory of Lyapunov function under demand of 7000 vehicles per hour.

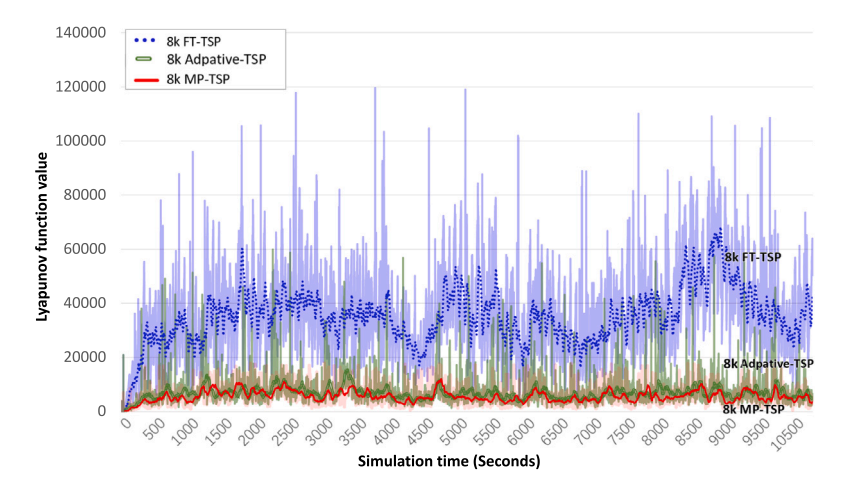


Fig. 11. Trajectory of Lyapunov function under demand of 8000 vehicles per hour.

better than the adaptive signal control integrated with transit signal priority and a given fixed-time signal controller integrated with transit signal priority at different demand settings.

We also care about the bus travel time in the downtown area after implementing max-pressure control and transit signal priority. We compare a given fixed time controller without considering transit signal priority (referred to as FT-noTSP), the origin max-pressure signal control (referred to as MP-noTSP, which is Varaiya's version), adaptive-TSP, FT-TSP, and MP-TSP. The results are shown in Fig. 13. As the demand increases, bus average travel time in the downtown area increases under both 5 traffic signal controllers. Bus average travel time is highest under the FT-noTSP controller, and MP-noTSP controller can reduce bus average travel time in the downtown area, but it is not the best. Moreover, without transit signal priority (FT-noTSP and MP-noTSP), bus average travel time in the downtown area is larger than the bus travel time under the traffic signal controller with transit signal priority (FT-TSP, Adaptive-TSP, and MP-TSP). Unsurprisingly, Adaptive-TSP is the second-best, since it is more "advanced" based on more loop detectors compared with FT-TSP, FT-noTSP, and MP-noTSP. Finally, we find that MP-TSP can reduce bus travel times in the downtown area, and both bus departure interval setting is 20 min in the comparisons. Table 3 provides details of the output of experiments. It is worthwhile to mention that at the start points of the bus lanes, where the upstream intersections are operated by the origin max-pressure controllers, there may be long bus waiting times as demand increases. This could reduce the MP-TSP travel time performance at the network level.

5.3. Impacts on the nearby roads

How the TSP influences nearby private vehicle roads and intersections are also worth exploring. Previous studies found that TSP may increase some delay for non-transit modes in the urban network, which inspires us to figure out how MP-TSP will influence nearby private vehicle roads. We calculate how the TSP influences the private vehicle links that are parallel to the bus links, which

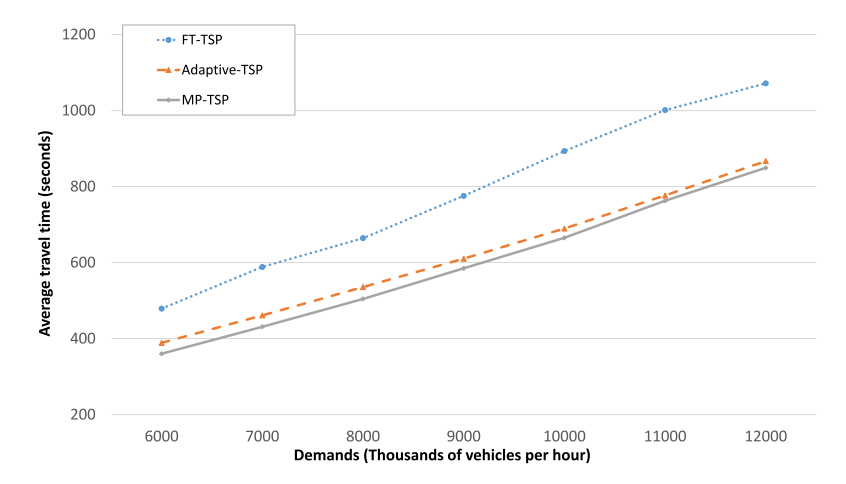


Fig. 12. Average travel time.

Table 2
Average travel time between MP-TSP, Adaptive-TSP, and FT-TSP.

Demands	FT-TSP (seconds)	Adaptive-TSP (seconds)	MP-TSP (seconds)
6000	478.71	388.60	360.07
7000	588.50	460.96	431.15
8000	664.24	535.55	504.23
9000	775.49	610.26	584.88
10000	893.26	689.60	665.15
11 000	1001.21	776.57	762.65
12000	1071.39	866.85	849.31

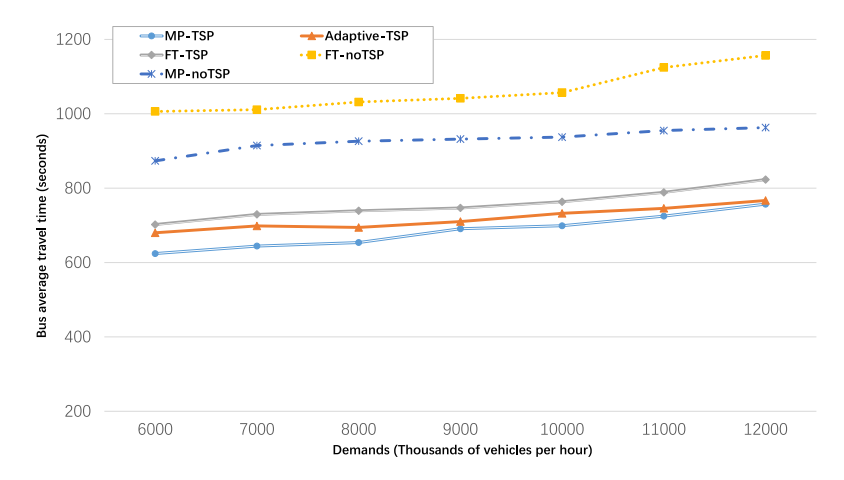


Fig. 13. Bus average travel time.

Table 3Bus average travel time (seconds) in downtown area.

Demands	MP-TSP	Adaptive-TSP	FT-TSP	MP-noTSP	FT-noTSP
6000	624.14	680.38	702.25	873.45	1006.31
7000	644.30	698.38	729.40	914.64	1011.02
8000	653.83	694.29	739.20	926.31	1031.59
9000	690.79	710.24	746.79	931.93	1041.52
10000	699.04	732.30	763.47	937.32	1057.03
11 000	724.85	745.69	788.66	954.89	1124.51
12000	757.18	766.85	823.18	962.90	1156.84

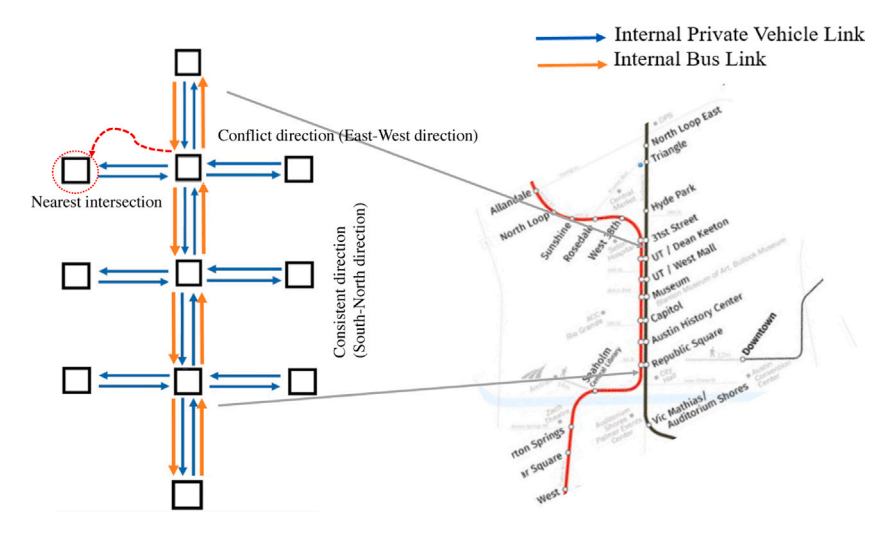


Fig. 14. Experimental diagram.

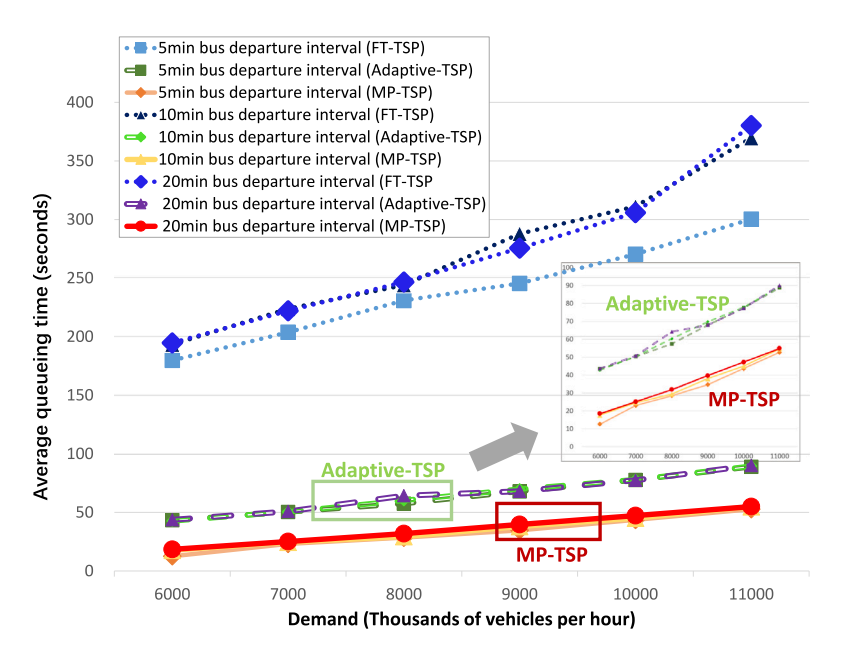


Fig. 15. Consistent direction.

are denoted as the consistent direction in Fig. 14, and the direction without bus links, which are denoted as the conflict direction in Fig. 14. Note that for the conflict directions, we only consider the links between the nearest next intersection. We use the average queueing time of private vehicles to figure out how FT-TSP, Adaptive-TSP, and MP-TSP influence the performance in those directions. Experimental setting details are shown in Fig. 14.

The results are shown in Figs. 15, 16, Tables 4, and 5. For the consistent direction, the MP-TSP has a significantly lower queueing time compared with FT-TSP and Adaptive-TSP when the private vehicle demand increases. For instance, when the demand is 11000 private vehicles per hour, the average queueing time when implementing MP-TSP is between 50 to 60 s under different bus departure intervals, but the average queueing time when implementing Adaptive-TSP is between 80 to 90 s. Furthermore, when the demand grows larger, the queueing time of FT-TSP increases faster than the queueing time of MP-TSP. These results are consistent with the property of MP-TSP because max-pressure control can serve as much demand as possible while giving priority to bus rapid transit. When the bus rapid transit departure interval is smaller, the consistent direction has lower queueing time, since buses arrive more frequently when their departure time gap is smaller.

As for the conflicting direction, when the demand is below 10 000 private vehicles per hour, MP-TSP is slightly better than FT-TSP when considering the queueing time. When the demand increases, MP-TSP is slightly worse than FT-TSP, because the max-pressure

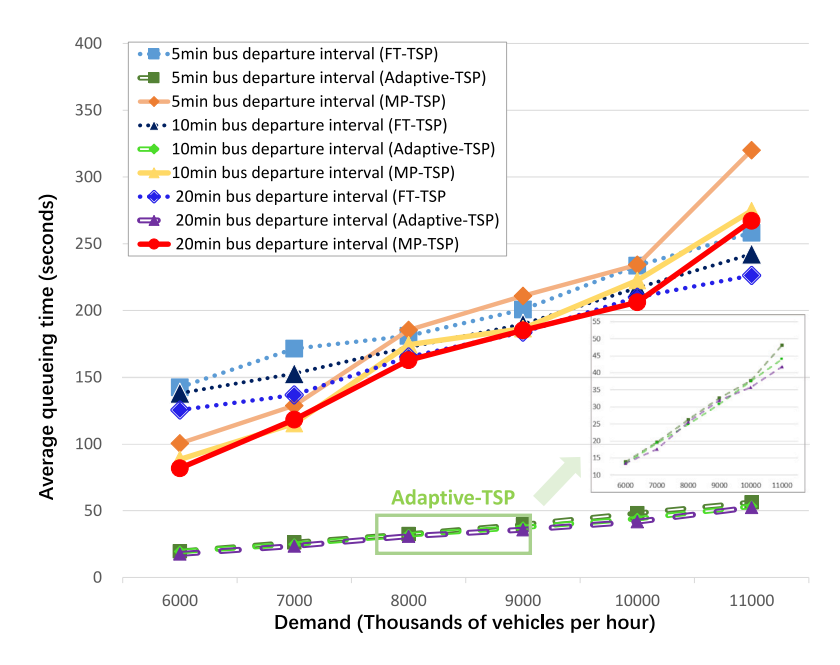


Fig. 16. Conflict direction.

Table 4
Average queueing time of private vehicles among FT-TSP, Adaptive-TSP, and MP-TSP and FT-TSP in the consistent direction.

5 min bus headway		
FT-TSP (seconds)	Adaptive-TSP (seconds)	MP-TSP (Seconds)
179.75	42.36	12.57
203.76	50.35	23.12
230.89	57.50	27.44
245.46	67.95	34.69
270.35	76.61	43.61
299.34	88.93	52.73
10 min bus headway		
FT-TSP (seconds)	Adaptive-TSP (seconds)	MP-TSP (Seconds)
193.24	42.68	17.62
223.75	50.50	24.57
244.03	60.24	29.34
287.86	69.81	37.97
311.15	77.96	45.03
369.52	89.47	54.77
20 min bus headway		
FT-TSP (seconds)	Adaptive-TSP (seconds)	MP-TSP (Seconds)
194.65	44.68	18.47
222.11	51.80	25.11
246.69	63.27	31.84
275.57	69.06	39.66
305.85	78.40	47.29
380.23	90.07	54.94

controller would give priority to bus phases and high demand approaches, which may cause some delay for conflicting movements. Furthermore, Adaptive-TSP performs best for the conflicting direction, because the adaptive signal controller can adjust its phase duration based on the dynamic private vehicle demands, but MP-TSP will give more priority for private vehicles on the consistent directions, which is the main transit corridor in the downtown Austin network. However, the travel time of private vehicles and buses at the network level indicates that this will not influence that MP-TSP has better performance than FT-TSP and Adaptive-TSP. When the bus departure interval is smaller, the conflict direction has a larger queueing time, because the consistent direction has more priority when buses arrive more frequently in the consistent direction.

Table 5Average queueing time of private vehicles among FT-TSP, Adaptive-TSP, and MP-TSP and FT-TSP in the conflict direction.

5 min bus headway		
FT-TSP (seconds)	Adaptive-TSP (seconds)	MP-TSP (Seconds)
142.40	13.91	100.39
171.39	19.63	128.73
181.00	26.29	185.36
200.67	32.53	210.92
233.56	37.62	234.21
258.25	48.31	320.09
10 min bus headway		
FT-TSP (seconds)	Adaptive-TSP (seconds)	MP-TSP (Seconds)
139.02	13.42	88.39
152.67	19.42	115.28
172.50	24.82	174.28
189.70	30.86	186.40
216.98	37.59	222.50
242.30	43.89	274.77
20 min bus headway		
FT-TSP (seconds)	Adaptive-TSP (seconds)	MP-TSP (Seconds)
125.42	13.55	81.71
136.67	17.56	118.17
165.20	25.56	162.78
188.00	31.86	185.10
214.00	35.71	206.13
226.22	41.77	267.21

6. Conclusions

In previous studies, max-pressure control only considered the private vehicle network. However, the urban transportation network also includes other traffic modes. Chen et al. (2020) extended max-pressure signal controller to autonomous vehicles and pedestrians for the first time. To boost the scope of the application of the max-pressure control policy, we propose a modified max-pressure control policy, which considers the transit signal priority of the bus rapid transit system. We analytically proved that the MP-TSP can still achieve maximum stability.

Numerical results in the downtown Austin network suggest that, although the modified max-pressure control policy will have a lower stable region compared with the original max-pressure control policy, it will have much lower bus travel time. Also, the modified max-pressure control policy performs better than the other fixed time signal control incorporating with transit signal priority and adaptive signal control incorporating transit signal priority based on the average number of waiting private vehicles, the trajectory of the proposed Lyapunov function, the average travel time of private vehicles, and the bus average travel time. When the private vehicle links are parallel to the bus links (consistent directions), the average queueing time increase with increase of bus departure intervals, and the MP-TSP performs better than the FT-TSP and Adaptive-TSP (the second-best one). On the other hand, for the direction conflicting with bus links, the MP-TSP performs better than FT-TSP when demand is low, and the average queueing time decreases with the increase of bus departure intervals. It should be noted that Adaptive-TSP performs best in the conflict direction with bus links, this is because the adaptive signal controller can adjust its phase duration based on the dynamic private vehicle demands, but MP-TSP will give more priority for private vehicles on the consistent directions because of the arrivals of buses. We also notice that at the start points of bus lanes, where the upstream intersections are operated by origin max-pressure signal controllers, there may be a long bus waiting time as demand increases, which could reduce MP-TSP travel time performance at the network level. Overall, the proposed modified max-pressure policy can serve more private vehicle demand and reduce travel time while including transit signal priority at the urban network level, which is more friendly to multi-modal traffic operations.

In the future, there are many extensions to consider. For example, streets comprise more than 80% of public space in cities, but they often fail to provide their surrounding communities with enough space where people can safely walk, bicycle, drive, take public transit, and socialize. Incorporating all of these modes into the max-pressure signal control scheme is an interesting and important challenge. Also, since the proposed signal control policy is non-cyclic, which means it will actuate phases in arbitrary orders when there is no bus arrives. Therefore, it would be interesting to study the performance with cyclic-based max pressure policy integrating with transit signal priority (Levin et al., 2020). In addition, the results will benefit from additional numerical analyses on the design of exclusive bus lanes, such as the layout of bus lanes, the number of bus lanes, location of bus lanes with regard to the different levels of private vehicle demand. Finally, it would benefit more when we consider the existence of connected and autonomous vehicles, which would help us develop a coordination approach combined with the proposed MP-TSP policy in the future.

CRediT authorship contribution statement

Te Xu: Conception, Methodology, Software and simulation, Visualization, Analysis and interpretation of results, Draft manuscript preparation, Validation, Writing – review & editing. **Simanta Barman:** Methodology, Software and simulation, Analysis and interpretation of results, Draft manuscript preparation, Validation. **Michael W. Levin:** Conception, Methodology, Visualization, Analysis and interpretation of results, Draft manuscript preparation, Validation, Writing – review & editing, Supervision, Funding acquisition. **Rongsheng Chen:** Software and simulation, Draft manuscript preparation, Validation. **Tianyi Li:** Draft manuscript preparation, Validation.

Acknowledgments

The authors gratefully acknowledge the support of the National Science Foundation, Award No. 1935514 and the support of Hsiao Shaw-Lundquist Fellowship of the University of Minnesota China Center. The authors also thanked the anonymous reviewers for their precious advice during the review process. All authors reviewed the results and approved the final version of the manuscript.

References

Anderson, P., Daganzo, C.F., 2020. Effect of transit signal priority on bus service reliability. Transp. Res. B 132, 2-14.

Bayrak, M., Guler, S.I., 2020. Determining optimum transit signal priority implementation locations on a network. Transp. Res. Rec. 2674 (10), 387-400.

Chang, J., Collura, J., Dion, F., Rakha, H., 2003. Evaluation of service reliability impacts of traffic signal priority strategies for bus transit. Transp. Res. Rec. 1841 (1), 23–31.

Chen, R., Hu, J., Levin, M.W., Rey, D., 2020. Stability-based analysis of autonomous intersection management with pedestrians. Transp. Res. C 114, 463–483. Chiabaut, N., Barcet, A., 2019. Demonstration and evaluation of an intermittent bus lane strategy. Public Transp. 11 (3), 443–456.

Chiabaut, N., Xie, X., Leclercq, L., 2012. Road capacity and travel times with bus lanes and intermittent priority activation: analytical investigations. Transp. Res. Rec. 2315 (1), 182–190.

Christofa, E., Papamichail, I., Skabardonis, A., 2013. Person-based traffic responsive signal control optimization. IEEE Trans. Intell. Transp. Syst. 14 (3), 1278–1289. Christofa, E., Skabardonis, A., 2011. Traffic signal optimization with application of transit signal priority to an isolated intersection. Transp. Res. Rec. 2259 (1), 192–201.

Claudel, C.G., Bayen, A.M., 2010a. Lax-Hopf based incorporation of internal boundary conditions into Hamilton-Jacobi equation. Part I: Theory. IEEE Trans. Autom. Control 55 (5), 1142–1157.

Claudel, C.G., Bayen, A.M., 2010b. Lax-Hopf based incorporation of internal boundary conditions into Hamilton-Jacobi equation. Part II: Computational methods. IEEE Trans. Autom. Control 55 (5), 1158-1174.

Currie, G., Lai, H., 2008. Intermittent and dynamic transit lanes: Melbourne, Australia, experience. Transp. Res. Rec. 2072 (1), 49-56.

Currie, G., Shalaby, A., 2008. Active transit signal priority for streetcars: experience in Melbourne, Australia, and Toronto, Canada. Transp. Res. Rec. 2042 (1), 41–49.

Deng, T., Nelson, J.D., 2011. Recent developments in bus rapid transit: a review of the literature. Transp. Rev. 31 (1), 69-96.

Ding, J., Yang, M., Wang, W., Xu, C., Bao, Y., 2015. Strategy for multiobjective transit signal priority with prediction of bus dwell time at stops. Transp. Res. Rec. 2488 (1), 10–19.

Dion, F., Rakha, H., Zhang, Y., 2004. Evaluation of potential transit signal priority benefits along a fixed-time signalized arterial. J. Transp. Eng. 130 (3), 294–303.

Eichler, M., Daganzo, C.F., 2006. Bus lanes with intermittent priority: Strategy formulae and an evaluation. Transp. Res. B 40 (9), 731-744.

Gregoire, J., Qian, X., Frazzoli, E., De La Fortelle, A., Wongpiromsarn, T., 2014. Capacity-aware backpressure traffic signal control. IEEE Trans. Control Netw. Syst. 2 (2), 164–173.

Hunter-Zaworski, K.M., Kloos, W.C., Danaher, A.R., 1995. Bus priority at traffic signals in Portland: the Powell Boulevard pilot project. Transp. Res. Rec. (1503). Levin, M.W., Hu, J., Odell, M., 2020. Max-pressure signal control with cyclical phase structure. Transp. Res. C 120, 102828.

Levin, M.W., Rey, D., Schwartz, A., 2019. Max-pressure control of dynamic lane reversal and autonomous intersection management. Transp. B 7 (1), 1693–1718. Levinson, H.S., Zimmerman, S., Clinger, J., Rutherford, G.S., 2002. Bus rapid transit: An overview. J. Public Transp. 5 (2), 1.

Li, L., Okoth, V., Jabari, S.E., 2021. Backpressure control with estimated queue lengths for urban network traffic. IET Intell. Transp. Syst. 15 (2), 320-330.

Li, M., Yin, Y., Zhang, W.-B., Zhou, K., Nakamura, H., 2011. Modeling and implementation of adaptive transit signal priority on actuated control systems. Comput.-Aided Civ. Infrastruct. Eng. 26 (4), 270–284.

Lin, Y., Yang, X., Zou, N., 2019. Passive transit signal priority for high transit demand: model formulation and strategy selection. Transp. Lett. 11 (3), 119–129. Lin, Y., Yang, X., Zou, N., Franz, M., 2015. Transit signal priority control at signalized intersections: a comprehensive review. Transp. Lett. 7 (3), 168–180.

Lopez, P.A., Behrisch, M., Bieker-Walz, L., Erdmann, J., Flötteröd, Y.-P., Hilbrich, R., Lücken, L., Rummel, J., Wagner, P., Wießner, E., 2018. Microscopic traffic simulation using SUMO. In: The 21st IEEE International Conference on Intelligent Transportation Systems. IEEE, URL https://elib.dlr.de/124092/.

Ma, W., Head, K.L., Feng, Y., 2014. Integrated optimization of transit priority operation at isolated intersections: A person-capacity-based approach. Transp. Res. C 40, 49–62.

Mercader, P., Uwayid, W., Haddad, J., 2020. Max-pressure traffic controller based on travel times: An experimental analysis. Transp. Res. C 110, 275-290.

Rey, D., Levin, M.W., 2019. Blue phase: Optimal network traffic control for legacy and autonomous vehicles. Transp. Res. B 130, 105-129.

Stevanovic, J., Stevanovic, A., Martin, P.T., Bauer, T., 2008. Stochastic optimization of traffic control and transit priority settings in VISSIM. Transp. Res. C 16 (3), 332–349.

Sun, X., Yin, Y., 2018. A simulation study on max pressure control of signalized intersections. Transp. Res. Rec. 2672 (18), 117-127.

Tassiulas, L., Ephremides, A., 1990. Stability properties of constrained queueing systems and scheduling policies for maximum throughput in multihop radio networks. In: 29th IEEE Conference on Decision and Control. IEEE, pp. 2130–2132.

Truong, L.T., Sarvi, M., Currie, G., 2016. An investigation of multiplier effects generated by implementing queue jump lanes at multiple intersections. J. Adv. Transp. 50 (8), 1699–1715.

Varaiya, P., 2013. Max pressure control of a network of signalized intersections. Transp. Res. C 36, 177-195.

Wadjas, Y., Furth, P.G., 2003. Transit signal priority along arterials using advanced detection. Transp. Res. Rec. 1856 (1), 220-230.

Wu, J., Ghosal, D., Zhang, M., Chuah, C.-N., 2017. Delay-based traffic signal control for throughput optimality and fairness at an isolated intersection. IEEE Trans. Veh. Technol. 67 (2), 896–909.

Wu, K., Lu, M., Guler, S.I., 2020. Modeling and optimizing bus transit priority along an arterial: A moving bottleneck approach. Transp. Res. C 121, 102873.

Wuthishuwong, C., Traechtler, A., 2013. Vehicle to infrastructure based safe trajectory planning for autonomous intersection management. In: 2013 13th International Conference on ITS Telecommunications (ITST). IEEE, pp. 175–180.

Xiao, N., Frazzoli, E., Li, Y., Wang, Y., Wang, D., 2014. Pressure releasing policy in traffic signal control with finite queue capacities. In: 53rd IEEE Conference on Decision and Control. IEEE, pp. 6492–6497.

Yang, K., Menendez, M., Guler, S.I., 2019. Implementing transit signal priority in a connected vehicle environment with and without bus stops. Transp. B 7 (1),

Zhou, G., Gan, A., 2005. Performance of transit signal priority with queue jumper lanes. Transp. Res. Rec. 1925 (1), 265-271.